Cell Reports

Article

Combinatorial genetic engineering strategy for immune protection of stem cell-derived beta cells by chimeric antigen receptor regulatory T cells

Graphical abstract

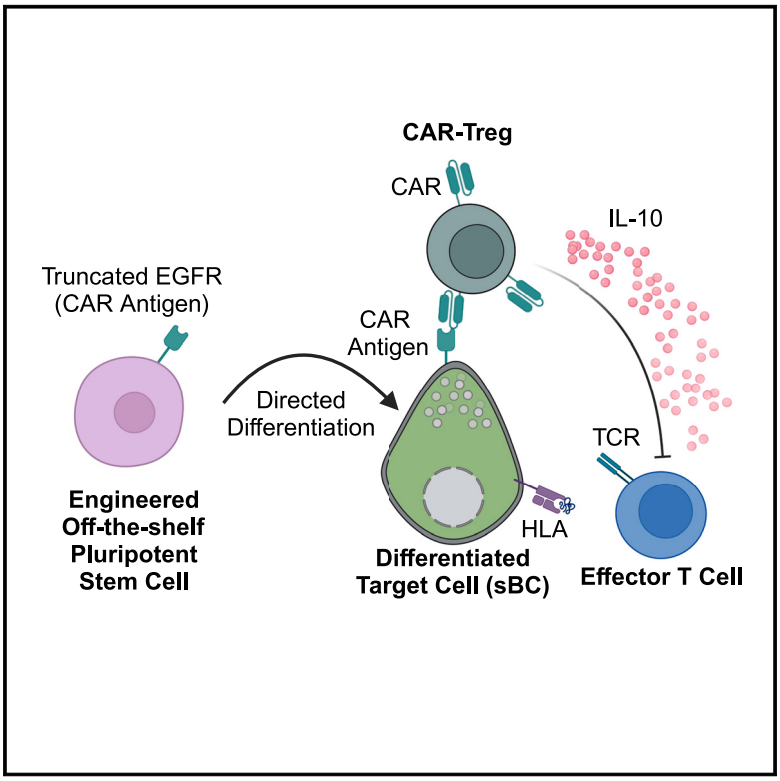

Authors

Jessie M. Barra, Rob A. Robino, Roberto Castro-Gutierrez, James Proia, Holger A. Russ, Leonardo M.R. Ferreira

Correspondence

holger.russ@ufl.edu (H.A.R.), ferreirl@musc.edu (L.M.R.F.)

In brief

Immune protection of human pluripotent stem cell (hPSC)-derived grafts remains a key hurdle in regenerative medicine. Barra and Robino et al. engineered hPSCs to express an inert bait protein and bait-specific immunosuppressive chimeric antigen receptor regulatory T cells (CAR-Tregs), accomplishing localized hPSC-derived beta cell immune protection in humanized mice.

Highlights

- Gene editing of human pluripotent stem cells (hPSCs) to express unique bait protein
- Regulatory T cell engineering with bait-specific chimeric antigen receptor (CAR-Treg)
- CAR-Tregs are suppressive *in vitro* when activated by bait-expressing cells
- CAR-Tregs protect bait-expressing hPSC-derived beta cells from immune destruction *in vivo*

Barra et al., 2024, Cell Reports *43*, 114994
November 26, 2024
https://doi.org/10.1016/j.celrep.2024.114994

CellPress

Cell Reports

CellPress
OPEN ACCESS

Article

Combinatorial genetic engineering strategy for immune protection of stem cell-derived beta cells by chimeric antigen receptor regulatory T cells

Jessie M. Barra,[1,2,6] Rob A. Robino,[3,4,5,6] Roberto Castro-Gutierrez,[1,2] James Proia,[1,2] Holger A. Russ,[1,2,7,*] and Leonardo M.R. Ferreira[3,4,5,7,8,*]

[1]Diabetes Institute, University of Florida, Gainesville, FL 32610, USA
[2]Department of Pharmacology and Therapeutics, University of Florida, Gainesville, FL 32610, USA
[3]Department of Microbiology and Immunology, Medical University of South Carolina, Charleston, SC 29425, USA
[4]Department of Regenerative Medicine and Cell Biology, Medical University of South Carolina, Charleston, SC 29425, USA
[5]Hollings Cancer Center, Medical University of South Carolina, Charleston, SC 29425, USA
[6]These authors contributed equally
[7]These authors contributed equally
[8]Lead contact
*Correspondence: holger.russ@ufl.edu (H.A.R.), ferreirl@musc.edu (L.M.R.F.)
https://doi.org/10.1016/j.celrep.2024.114994

SUMMARY

Regenerative medicine is a rapidly expanding field harnessing human pluripotent stem cell (hPSC)-derived cells and tissues to treat many diseases, including type 1 diabetes. However, graft immune protection remains a key challenge. Chimeric antigen receptor (CAR) technology confers new specificities to effector T cells and immunosuppressive regulatory T cells (Tregs). One challenge in CAR design is identifying target molecules unique to the cells of interest. Here, we employ combinatorial genetic engineering to confer CAR-Treg-mediated localized immune protection to stem cell-derived cells. We engineered hPSCs to express truncated epidermal growth factor receptor (EGFRt), a biologically inert and generalizable target for CAR-Treg homing and activation, and generated CAR-Tregs recognizing EGFRt. Strikingly, CAR-Tregs suppressed innate and adaptive immune responses *in vitro* and prevented EGFRt-hPSC-derived pancreatic beta-like cell (sBC [stem cell-derived beta cell]) graft immune destruction *in vivo*. Collectively, we provide proof of concept that hPSCs and Tregs can be co-engineered to protect hPSC-derived cells from immune rejection upon transplantation.

INTRODUCTION

Stem cell-derived tissues have the potential to revolutionize the field of regenerative medicine, with multiple trials ongoing.[1] However, many of these studies rely on systemic immune suppression, which exposes patients to many secondary complications, such as viral infections, nephrotoxicity, neurotoxicity, and hyperglycemia, thus excluding a large patient population.[2–4]

Regulatory T cells (Tregs) are extremely effective immunosuppressive cells, combining over a dozen known mechanisms to inhibit immune responses, including immunosuppressive soluble factor production, interleukin-2 (IL-2) sequestration, receptor-mediated inhibition, and modulation of antigen-presenting cells to suppress effector T cell (Teff) activation.[5–7] Tregs are thus an attractive target for manipulation to induce or restore immune tolerance, potentially circumventing the need for systemic suppression commonly employed in transplant recipients. Human Tregs can be isolated, expanded, and reinfused into patients. However, because of the relatively low frequency of antigen-specific Tregs, utilizing naturally occurring Tregs as a therapeutic population in the clinic has proven challenging.[8–10] Preclinical disease models show that antigen-specific Tregs are more efficacious than expanded polyclonal Tregs at suppressing immune responses.[11,12] Therefore, conferring desired antigen specificity to patient-derived polyclonal Tregs may represent an efficacious approach to induce immune tolerance while preventing off-target immune suppression.

Chimeric antigen receptor (CAR) technology has shown great promise in its ability to redirect T cell responses toward a target antigen.[13] A CAR is a hybrid protein that includes an antigen-binding domain of a specific antibody that is then fused to a transmembrane domain and T cell activation intracellular domains derived from the T cell receptor (TCR) CD3 signaling complex and costimulatory receptors.[14] CD19 CAR-T cells have displayed great effectiveness for targeting of B cell leukemias and lymphomas.[15,16] Harnessing CAR technology to redirect Treg specificity could therefore enhance localized immune tolerance toward a specific antigen of interest without impairing systemic immune responses to future pathogens.[17] Developing antigen-targeted CAR-Tregs to inhibit autoreactive Teff responses is an

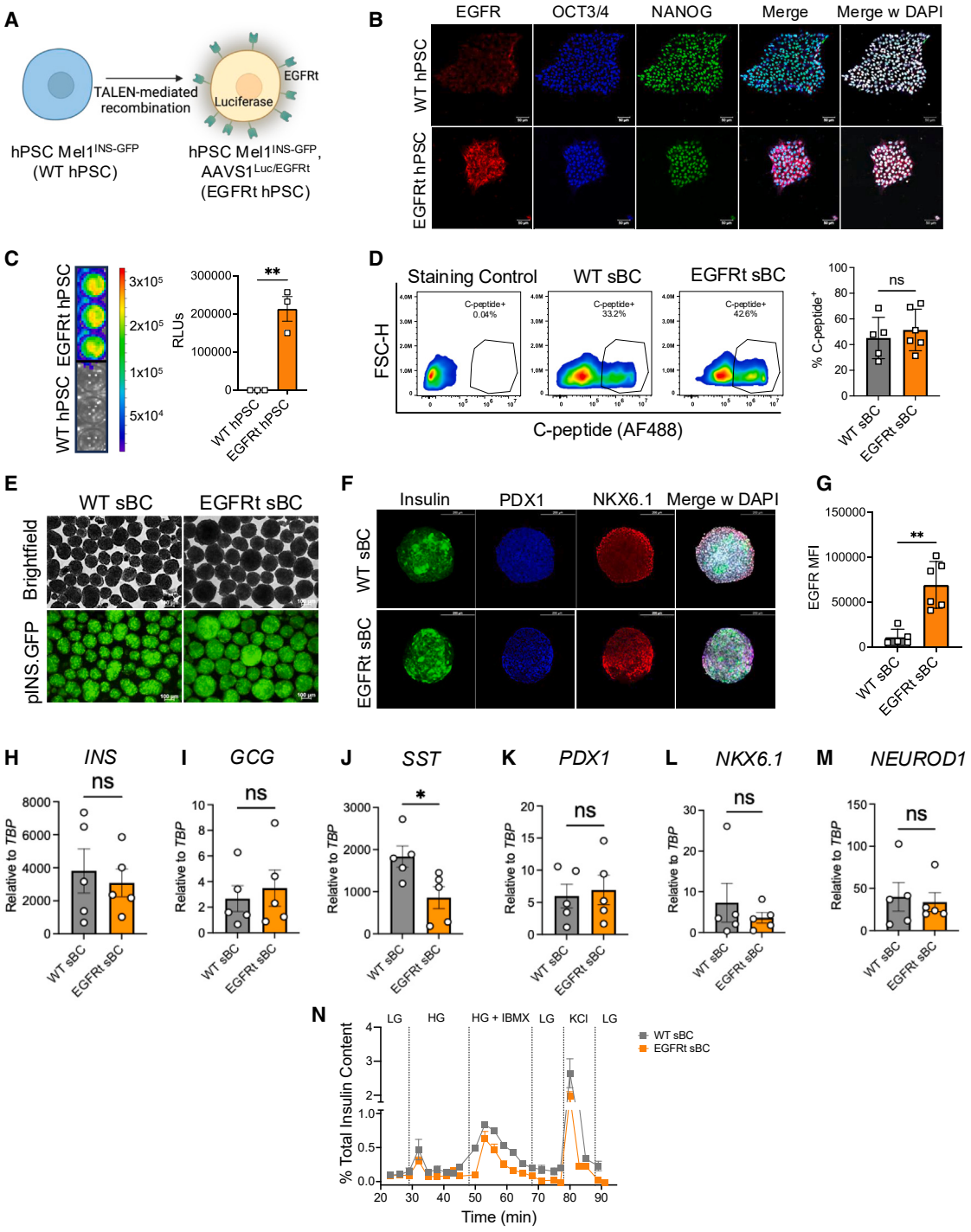

Figure 1. Genetically engineered EGFRt-hPSCs efficiently differentiate into stem cell-derived beta cells

(A) Schematic for TALEN-mediated genome recombination for insertion of constitutive luciferase reporter and EGFRt constructs into Mel1$^{INS-GFP}$ hPSC line.

(B) Immunofluorescence staining for EGFR/EGFRt (red), OCT3/4 (blue), NANOG (green), and DAPI (white) in WT or EGFRt-hPSCs at 20× magnification. Scale bars represent 50 μm.

(C) Representative luciferase assay and quantification (n = 3 technical replicates) of relative light units (RLUs) in WT and EGFRt-hPSCs. Bars represent mean and standard deviation.

(D) Flow cytometry of C-peptide expression on day 23 of differentiation in WT and EGFRt-sBCs (n = 6 biological replicates). Bars represent mean and standard deviation.

(legend continued on next page)

attractive therapeutic strategy for preventing graft destruction and has been applied in preclinical models of autoimmunity and transplantation rejection.[18–22] However, these therapies are only effective if the CAR is directed against a unique protein expressed by target cells and ideally no other tissues.

One disease in which the use of regenerative medicine and CAR-Tregs is of great interest is type 1 diabetes (T1D), which results from the specific destruction of insulin-producing pancreatic beta cells by the patient's immune system. Patients with T1D rely on exogenous insulin to maintain glycemic control. However, this approach is imperfect, leaving patients at risk for hypoglycemic episodes and multiple secondary complications, including cardiovascular disease, retinopathy, neuropathy, and renal failure.[23] Beta cell replacement strategies such as islet or pancreas transplantation represent a promising alternative approach to restore glucose homeostasis and prevent life-threatening hypoglycemic unawareness events, but widespread use is limited by donor organ availability and immune-mediated rejection.[24] To make beta cell replacement a feasible treatment option for all patients with T1D, both challenges must be addressed. The generation of insulin-producing beta-like cells from human pluripotent stem cells (hPSC) sources can now overcome the limited supply and quality of cadaveric donor organs, supplying unlimited numbers of stem cell-derived beta cells (sBCs).[25–28] The use of sBCs is currently under investigation in a phase 1/2 clinical trial (ClinicalTrials.gov: NCT04786262) in conjugation with systemic immune suppression. A key remaining challenge is the need to overcome immune rejection of sBCs after transplantation.

Here, we harness genome engineering of hPSCs to induce the expression of a truncated form of the epidermal growth factor receptor (EGFRt). This biologically inert protein serves as a generalizable, proof-of-principle target for CAR-Treg homing and localized activation and, importantly, is not naturally expressed on any other tissues. We demonstrate that EGFR CAR-Tregs are activated by EGFRt-expressing cells and can inhibit innate and adaptive immune responses *in vitro* while maintaining Treg identity. To test the efficacy of this approach in a disease setting, we differentiated engineered hPSCs to generate EGFRt-expressing sBCs. Importantly, CAR-Tregs suppressed Teff-mediated destruction of EGFRt-expressing sBCs transplanted into immunodeficient mice. Collectively, we provide *in vitro* and *in vivo* proof-of-concept data that hPSCs and Tregs can be co-engineered to specifically protect hPSC-derived cells expressing a unique truncated target protein from immune rejection upon transplantation. This proof-of-concept strategy can be adopted to other protein targets, allowing for the directed protection of a multitude of stem cell-derived tissues without off-target suppression of other immune responses, helping propel the expansion and implementation of regenerative medicine therapeutics across multiple diseases.

RESULTS

Genome engineering established EGFRt-hPSCs that can effectively differentiate into hPSC-derived beta-like cells

To test whether combinatorial cell engineering can be utilized to prevent immune rejection of a stem cell-derived cell type, we introduced a genetically encoded inert surface molecule in hPSCs. Our criteria for such a molecule were that it ought to be (1) expressed on the cell surface; (2) biologically inert, i.e., not transduce any signal to the expressing cell; (3) immunologically inert, i.e., not contain epitopes that would be recognized as foreign by the host immune system; and (4) not be expressed by any other cell types. To fulfill these criteria as a proof-of-concept study, we selected human EGFRt, which lacks the intracellular signaling domain and a large portion of the extracellular ligand binding domain. Using established protocols for Transcription Activator-Like Effector Nuclease (TALEN)-mediated site-specific genetic engineering of the AAVS1 locus in hPSCs,[29,30] we constitutively expressed EGFRt and Firefly luciferase genes in Mel1$^{INS\text{-}GFP}$ hPSCs (Figure 1A), which already contain a green fluorescence protein (GFP) reporter gene driven by the endogenous insulin promoter (pINS.GFP).[31] Immunofluorescence (IF) analysis revealed uniform expression of EGFRt in clonal colonies compared to control, wild-type (WT) colonies, while pluripotent stem cell markers OCT3/4 and NANOG were expressed at comparable levels (Figure 1B). Similarly, flow cytometry (FC) analysis demonstrated high EGFRt surface expression specifically in EGFRt-hPSCs (Figure S1A). Moreover, EGFRt-hPSCs, but not WT cells, exhibited readily detectable bioluminescence upon the addition of D-luciferin, indicating functional integration of the luciferase transgene (Figure 1C).

Next, we performed directed differentiation of EGFRt-hPSCs to generate stem cell-derived beta cells (sBCs) using established protocols.[29,30,32] Gross morphology of sBC clusters generated from either WT- or EGFRt-hPSCs throughout differentiation was comparable on days 0, 3, and 9 (Figure S1B). Compared to WT Mel1$^{INS\text{-}GFP}$ hPSCs and derived definitive endoderm (DE), EGFRt-hPSCs expressed equal levels of pluripotency markers SOX2 and TRA-1-60 (Figure S1C), and EGFRt-hPSC-derived DE expressed equal levels of DE markers SOX17 and FOXA2 (Figure S1D), as assessed by FC quantification prior to

(E) Representative live bright-field (BF) images of clusters on day 23 as well as the GFP insulin reporter (pINS.GFP) for WT and EGFRt-expressing cells. Scale bars represent 100 μm.

(F) Immunofluorescence staining of day 23 WT and EGFRt-sBCs for insulin (green), PDX1 (blue), and NKX6.1 (red) merged with DAPI (white). Scale bars represent 200 μm.

(G) Flow cytometry quantification of EGFR surface expression (MFI, mean fluorescence intensity) in WT and EGFRt-sBCs on day 23 (n = 6 biological replicates). Bars represent mean and standard deviation.

(H–M) Gene expression analysis of hormone genes *INS*, *GCG*, and *SST* and transcription factor genes *PDX1*, *NKX6.1*, and *NEUROD1* within WT and EGFRt-sBCs on day 23 (n = 5 biological replicates). Bars represent mean and standard error of the mean.

(N) Representative dynamic glucose-stimulated insulin secretion assay on day 30 in WT and EGFRt-sBC normalized to insulin content. Points represent mean and standard deviation (n = 3 biological replicates). Data are representative of at least 3 independent experiments.

All data were analyzed by unpaired t test. ns, not significant; $^{*}p < 0.05$ and $^{**}p < 0.01$.

and on day 3 of differentiation, respectively. Similarly, expression of day 9 pancreatic progenitor markers NKX6.1 and PDX1 was comparable between lines (Figure S1F). Live imaging of the pINS.GFP reporter and FC-based analysis of human C-peptide (a stable byproduct of endogenous insulin production) on day 23 of differentiation demonstrated comparable expression levels between both groups (Figures 1D and 1E). Additionally, both WT and EGFRt-sBCs displayed comparable high frequencies of PDX1$^+$ (Figure S1E), PDX1$^+$NKX6.1$^+$ (Figure S1G), and C-peptide$^+$NKX6.1$^+$ populations (Figure S1H). IF staining confirmed the expression of PDX1 and NKX6.1 within both WT and EGFRt-sBCs on day 23 (Figure 1F). FC analysis of EGFR expression confirmed that close to 100% of EGFRt-sBCs at day 23, but not WT controls, expressed high levels of surface EGFRt (Figures 1G and S1I). Gene expression analysis demonstrated no significant differences in expression of key islet hormone (Figures 1H–1J), transcription factor (Figures 1K–1M, S1J, and S1K), or beta cell function genes (Figure S1L–S1R), except for *SST* (Figure 1J), between WT and EGFRt-sBCs. Employing dynamic glucose-stimulated insulin secretion assays to assess the function of both WT- and EGFRt-sBCs directly showed similar functional responses to high glucose, as well as high glucose and IBMX, which triggers the amplifying pathway,[33] and depolarization by KCl (Figure 1N). Collectively, these data confirm that the addition of EGFRt and luciferase transgenes does not impair the directed differentiation efficiency or functionality of EGFRt-sBCs.

EGFR CAR-Tregs are stable and respond to EGFRt-expressing cells

Equipped with *bona fide* hPSCs, and the sBCs derived from them, expressing a unique inert surface marker EGFRt, we sought to generate immunosuppressive Treg populations recognizing EGFRt. To accomplish this, we introduced a CAR recognizing human EGFR and EGFRt[34] via lentivirus transduction in human CD4$^+$CD25^{hi}CD127$^-$ Tregs isolated via fluorescence-assisted cell sorting (FACS) from human peripheral blood (Figure 2A). We consistently achieved approximately 80% CAR transduction efficiency following Treg activation, lentiviral transduction, and expansion as measured by CAR mCherry reporter expression (Figure 2B). Modified Tregs exhibited high expression of the Treg lineage transcription factors FOXP3 and HELIOS compared with Teff controls, indicating a stable phenotype after CAR-Treg generation at day 9 (Figure 2C). To test the function of the EGFR-CAR, we co-cultured CAR-Tregs with anti-CD3/CD28 beads, WT K562 cells, or K562 cells overexpressing EGFRt. K562 cells are a human leukocyte antigen (HLA)-null, CD80/86$^-$ cell line and thus are not recognized by human T cells.[35] After 48 h of co-culture, we measured the surface expression of CD25, the high-affinity IL-2 receptor alpha chain, and CD71, the transferrin receptor, as a readout of Treg activation and observed their upregulation in CAR-Tregs co-incubated with EGFRt-expressing K562 cells or anti-CD3/CD28 bead controls but not WT K562 cells (Figure 2D). Treg identity in EGFRt-K562 or anti-CD3/CD28 bead-activated CAR-Tregs was largely preserved and comparable between groups, as assessed by the expression levels of FOXP3 and HELIOS after 9 days (Figure 2E). To further investigate the stability of CAR-Tregs, we performed repeated stimulation experiments using either anti-CD3/CD28 beads (endogenous TCR and CD28 activation) or irradiated EGFRt-K562 cells (CAR activation) and observed stable, high frequencies of FOXP3 and HELIOS double-positive cells even after two additional rounds of stimulation (Figures 2F and S2D). In addition, CAR-Tregs secreted negligible levels of interferon (IFN)γ, IL-17A, and IL-17F compared with CAR-Teff cells, irrespective of Treg mode of activation or round of stimulation (Figures S2E–S2G). These data demonstrate that CAR-Tregs remain stable following genetic modification and are activated specifically in the presence of EGFRt-expressing cells.

CAR-Tregs inhibit innate and adaptive immune activation when cultured with EGFRt-sBCs

Next, we assessed CAR-Treg function with cells of therapeutic interest, EGFRt-sBCs, by employing several co-culture assay systems. Quantification of activation markers CD71 and CD69 on the surface of CAR-Tregs by FC revealed significant upregulation when co-cultured with EGFRt-sBCs, as compared to untransduced (UT) Tregs (Figures 3A and 3B). This was also observed when CAR-Tregs were co-cultured with EGFRt-hPSCs (Figure S2A). Secretion levels of cytokines IL-10, associated with suppression of macrophages[36] and T cells,[37] and IL-13, associated with suppression of monocytes[38] and mesangial cells,[39] as well as protection of pancreatic islets,[40] were significantly increased when CAR-Tregs were cultured in the presence of EGFRt-sBCs (Figures 3C and 3D). In contrast, production of these cytokines was not induced in UT Treg controls. Interestingly, co-culture with UT Tregs or CAR-Tregs did not suppress MCP-1 (Figure 3E) secretion by sBCs, suggesting that CAR-Tregs do not impact sBC chemokine secretion and that potential immune infiltration of grafts *in vivo* may be facilitated by beta cell-derived signals. To confirm that our CAR-Tregs are not cytotoxic toward our sBCs once activated, we quantified the level of cleaved caspase-3 within pINS.GFP$^+$ cells. We observed no significant differences in the frequency of caspase 3$^+$ sBCs cultured with UT Tregs, UT Teffs, or CAR-Tregs (Figure 3F), while culture with CAR-Teffs demonstrated a robust increase in caspase 3 within sBCs. These data suggest that our Tregs can be functionally suppressive once activated by EGFRt-expressing cells without inducing sBC toxicity.

Since attenuation of dendritic cell (DC) maturation and stimulatory function is thought to be one of the main mechanisms through which Tregs inhibit immune responses,[6,7] we tested possible immune-suppressive effects of CAR-Tregs on monocyte-derived DCs (moDCs) in co-cultures with EGFRt-sBC-activated CAR-Tregs (Figure 3G). Compared to control moDCs cultured alone, the addition of either EGFRt-sBC-activated CAR-Tregs or anti-CD3/CD28 bead-activated UT Tregs downregulated CD80 and CD86 costimulatory receptor surface expression on moDCs (Figures 3H and S2C). Of note, EGFRt-hPSC-activated CAR-Tregs also downregulated these receptors in moDCs compared to controls (Figure S2B). However, when we assessed the secretion of pro-inflammatory DC cytokines IL-12p40 (Figure 3I) and IL-15 (Figure 3J), only co-cultures with CAR-Tregs displayed significantly reduced cytokine secretion. This observation, together with the fact that EGFRt-sBC-activated CAR-Tregs downregulated CD86 on moDCs to a greater

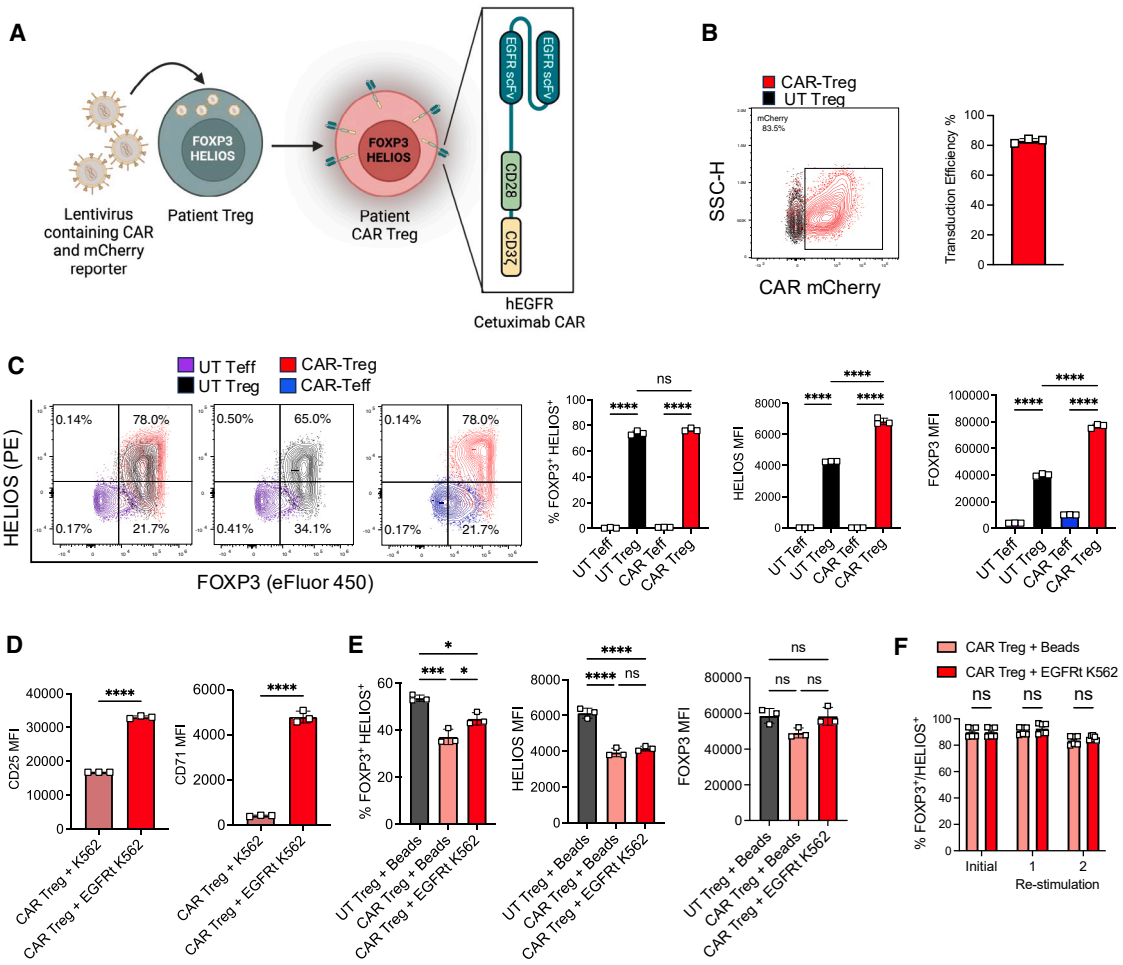

Figure 2. EGFR CAR-Tregs are stable after transduction and respond to EGFRt-expressing target cells

(A) EGFR-CAR construct and schematic for lentiviral CAR transduction approach into regulatory human T cells.

(B) Representative flow cytometry plot and quantification (N = 3 biological replicates) of transduction efficiency employing CAR mCherry reporter expression in untransduced (UT) and CAR-transduced regulatory T cells (Tregs). Bar represents mean and standard error of the mean.

(C) Flow cytometry and quantification of Treg identity marker HELIOS and FOXP3 expression in UT effector T cells (Teffs), UT Tregs, CAR-Teff cells, or CAR-Tregs. Bars represent mean and standard deviation (n = 3 technical replicates).

(D) Flow cytometry analysis of activation markers CD25 and CD71 expression on CAR-Tregs cultured with control (WT) or EGFRt-expressing K562 cells (n = 3 technical replicates). Bars represent mean and standard deviation.

(E) Quantification of flow cytometry data for FOXP3 and HELIOS expression 9 days after stimulation with anti-CD3/CD28 beads or EGFRt-K562 cells (n = 3 technical replicates). Bars represent mean and standard deviation.

(F) Flow cytometry analysis of FOXP3 and HELIOS expression in CAR-Tregs following repeated stimulation with either anti-CD3/CD28 beads or EGFRt-K562 cells (n = 6 technical replicates). Bars represents mean and standard deviation. Data are representative of at least 2 independent experiments.

Data were analyzed by two-way ANOVA with multiple comparisons in (C) and (E), unpaired t test for (D), or two-way ANOVA with multiple comparisons in (F). ns, not significant; *p < 0.05, **p < 0.01, ***p < 0.001, and ****p < 0.0001.

extent than anti-CD3/CD28-activated UT Tregs (Figure 3H), suggests that CAR-Tregs are more potent suppressors of DC function than polyclonally activated Tregs. Another predominant mechanism of Treg-mediated suppression is the inhibition of Teff proliferation, achieved by the sequestration of IL-2 via CD25 and secretion of the inhibitory cytokine IL-10.[6,7] Thus, we assessed the ability of activated CAR-Tregs to reduce Teff proliferation in co-culture assays with CAR-Tregs and CellTrace Far Red-stained CD4$^+$ and CD8$^+$ CAR-Teffs (Figure 3K). We observed a Treg:Teff ratio-dependent reduction in the proliferation of Teffs when CAR-Tregs were added (Figure 3L).

CAR-Tregs traffic to and suppress Teff-mediated destruction of EGFRt-sBC grafts

To determine if CAR-Tregs protect EGFRt-sBC grafts *in vivo*, we harnessed a humanized mouse model of sBC transplant rejection.[20,41] EGFRt-sBCs were transplanted into immune-deficient NSG mice and allowed to engraft and vascularize for 3 weeks, followed by immune challenge with either CAR-Teffs alone or

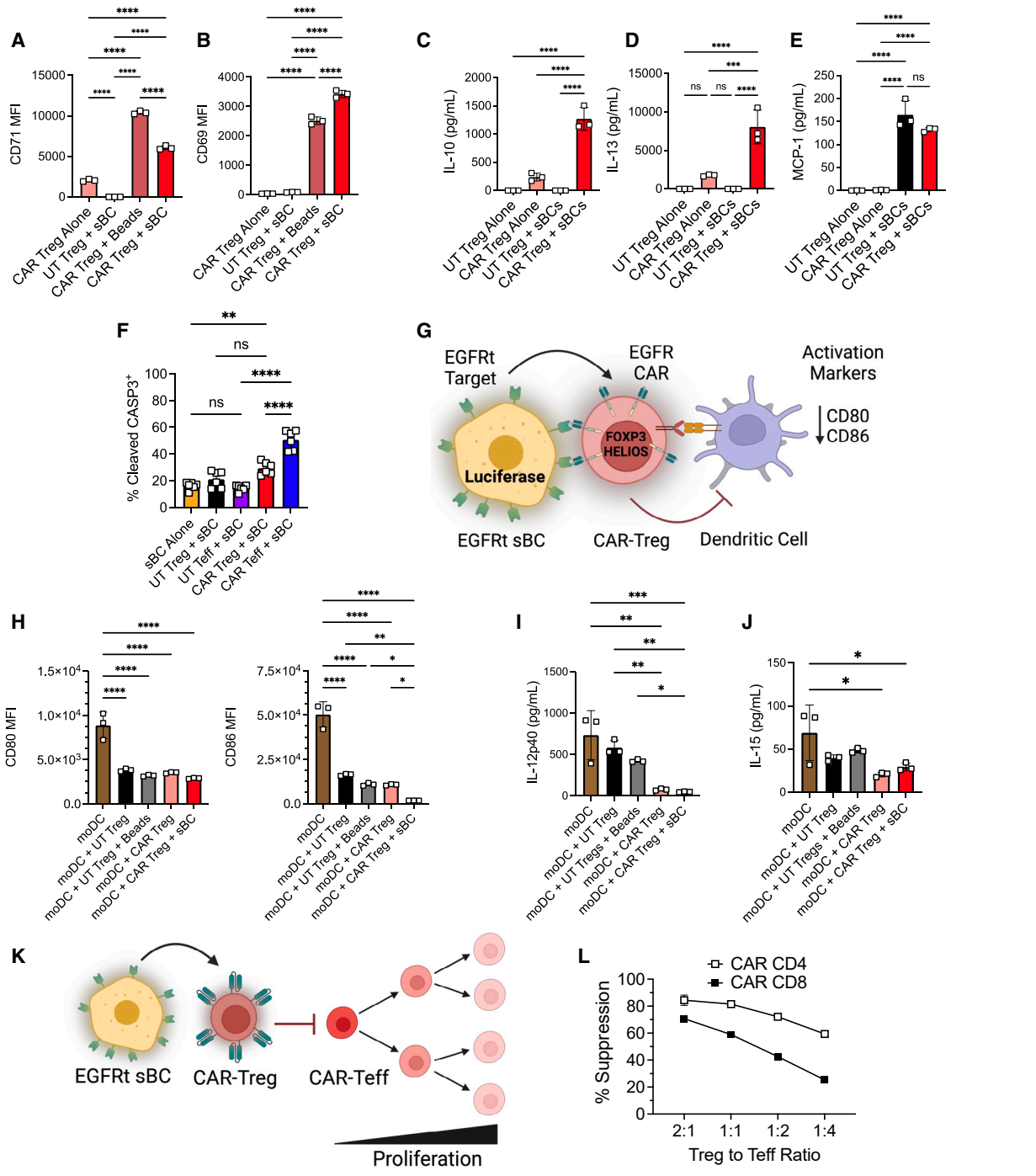

Figure 3. CAR-Tregs cultured with EGFRt-sBCs reduce dendritic cell responses and Teff proliferation

(A and B) Flow cytometry quantification of activation markers CD71 (A) and CD69 (B) expression in Tregs after 48-h co-culture with EGFRt-sBCs (n = 3 technical replicates). Bars represent mean and standard deviation.

(C–E) Quantification of IL-10 (C), IL-13 (D), and MCP-1 (E) protein levels in supernatants from co-cultures (n = 3 technical replicates). Bars represent mean and standard deviation.

(F) Flow cytometry quantification of cleaved caspase-3 frequency in sBCs after co-culture with UT (untransduced) Tregs, CAR-Tregs, UT Teffs, or CAR-Teffs (n = 6 technical replicates). Bars represent mean and standard deviation.

(G) Schematic for CAR-Treg suppression of monocyte-derived dendritic cells (moDCs) in co-culture.

(H) Flow cytometry analysis of CD80 and CD86 expression within $CD83^+$ moDCs (n = 3 technical replicates). Bars represent mean and standard deviation.

(legend continued on next page)

in combination with CAR-Tregs at a 1:2 ratio (Figure 4A). CAR-Teff infusion has been recently shown to be a robust method to induce effective rejection of transplanted beta cells in NSG mice without the aberrant development of graft-versus-host disease.[20,41] Utilizing the constitutive luciferase reporter, we performed longitudinal *in vivo* imaging of EGFRt-sBC grafts on subsequent days pre- and post-T cell infusion (Figure 4B). Strikingly, we observed that, in mice receiving CAR-Teffs alone, graft mass started to diminish at day 15 and was mostly undetectable by day 24, whereas luciferase signal was significantly maintained in mice co-infused with CAR-Tregs (p = 0.0013) (Figures 4C and 4D).

After 4 weeks *in vivo*, we recovered EGFRt-sBC grafts and spleens from mice of both experimental groups and performed IF staining and FC quantification of T cell populations. IF staining of grafts demonstrated the preservation of sBC cluster architecture with prominent insulin expression within the CAR-Treg-treated group, while nearly all insulin$^+$ cells were destroyed within CAR-Teff-only grafts (Figure 4E), confirming the bioluminescence quantification of graft persistence (Figures 4B–4D). We observed prominent T cell infiltrates marked by surface CD3 staining in both groups. However, 50% of the T cells within grafts of CAR-Treg-treated mice expressed the Treg marker FOXP3 and were found near and directly surrounding insulin-expressing sBC grafts (Figures 4E and 4F). Moreover, high EGFRt surface expression was readily observed on human sBC graft cells, as revealed by human nuclear antigen (HNA) co-staining (Figure 4G), and overlapped with insulin expression (Figure S3A), in addition to human immune cells also stained by HNA (Figure 4G). Quantification of the frequency of EGFR$^+$HNA$^+$ cells demonstrated significant maintenance of sBC graft mass (Figure 4H). Moreover, we found a marked reduction in the overall frequency of CD3$^+$HNA$^+$ T cells within the CAR-Treg-treated group (Figure 4I). We also confirmed a minimal presence of other populations within the graft, such as glucagon$^+$ alpha cells (Figure S3B), CK19$^+$ ductal cells (Figure S3C), SOX9$^+$ progenitors (Figure S3C), and SLC18A1$^+$ enterochromaffin cells (Figure S3D). Importantly, FC quantification revealed a significant increase in the frequency of human CD4$^+$ FOXP3$^+$ Tregs in spleens (Figure S3E) and grafts (Figure S3F) from mice that received both CAR-Teffs and CAR-Tregs compared to CAR-Teffs alone. These data indicate that CAR-Tregs home to and persist within EGFRt-sBC grafts and provide a localized immune-tolerant environment to protect transplanted cells in this preclinical animal model system.

DISCUSSION

Regenerative medicine focused on stem cell technology offers tremendous potential for the replacement of functional tissues to treat a host of different human diseases. Induced pluripotent stem cells (iPSCs) can be generated effectively in a patient-specific manner and can be used in a personalized fashion. However, challenges with patient-specific strategies are multifold, most critically the variability between patients and the iPSCs derived from them, long time requirements, and high cost. An attractive alternative approach is the generation of large numbers of "off-the-shelf" validated stem cell-derived tissues that would allow for economical and consistent use in a wide patient population at scale.[42] However, transplantation of cells derived from only one or a few stem cell lines would result in immune rejection in most patients, similar to solid organ transplantation, which is currently mitigated by systemic immune suppression. Indeed, currently ongoing sBC replacement therapy trials for patients with T1D rely on systemic immunosuppression, severely restricting the patient pool. Several groups have employed genetic engineering to alter the expression of key immune genes on stem cell-derived tissues, including polymorphic HLA molecules and immune checkpoint inhibitors to evade allogenic immune rejection[29,30,43–45] to overcome immune rejection. However, such hypoimmunogenic hPSC-derived tissues may not provide complete immune evasion due to the multitude of immune mechanisms driving rejection that need to be inhibited effectively. In addition, hypoimmunogenic cells also carry increased risks, as the lack of HLA and other immune surveillance mechanisms prevents effective cell clearance in the event of virus infection or cancer formation.[46] Of note, how exposure to an autoimmune environment could affect hypoimmunogenic cells is similarly unknown, largely due to the lack of appropriate human model systems.[47]

The immunosuppressive power of Tregs is unmatched, reeducating multiple arms of the immune system to induce long-term immune tolerance instead of only providing immune evasion. Therefore, targeting Tregs to protect a transplant is an attractive approach to generate a localized immunosuppressive environment. Indeed, Tregs have shown great promise for the treatment of autoimmune diseases and suppression of transplantation rejection.[8,48] However, there are remaining concerns related to CAR target specificity, longevity of suppressive ability, phenotype stability, and general safety.[49] Specific targeting of a CAR against a unique antigen that is not present elsewhere in the human body will assuage some of these concerns. The recent improvements in the generation of genetically engineered hPSCs and tissues derived from them deliver a unique opportunity to design CAR baits on target tissue that can be employed to provide localized immune tolerance via attracting CAR-Tregs.[50] Providing localized immune tolerance instead of immune evasion for stem cell-derived cell grafts might have distinct advantages by targeting multiple arms of the immune system simultaneously. Indeed, other groups have utilized genetic engineering approaches to target CAR-Tregs that specifically recognize a surface protein on target tissues. For instance, HLA-A2

(I and J) Quantification of IL-12p40 (I) and IL-15 (J) protein levels in supernatants from co-cultures with moDCs (n = 3 technical replicates). Bars represent mean and standard deviation.

(K) Schematic for CAR-Treg-mediated suppression of T responder (Tresp) cell proliferation after being stimulated by EGFRt-sBCs.

(L) Quantification of suppression of CAR CD4$^+$ (white boxes) or CAR CD8$^+$ (black boxes) Tresp cells compared to Tresp cells cultured alone at different Treg:Tresp cell ratios (n = 3 technical replicates). Points represent mean and standard deviation. Data are representative of at least 2 independent experiments.

Data were analyzed by one-way ANOVA with multiple comparisons (A–F and H–J). ns, not significant; *p < 0.05, **p < 0.01, ***p < 0.001, and ****p < 0.0001.

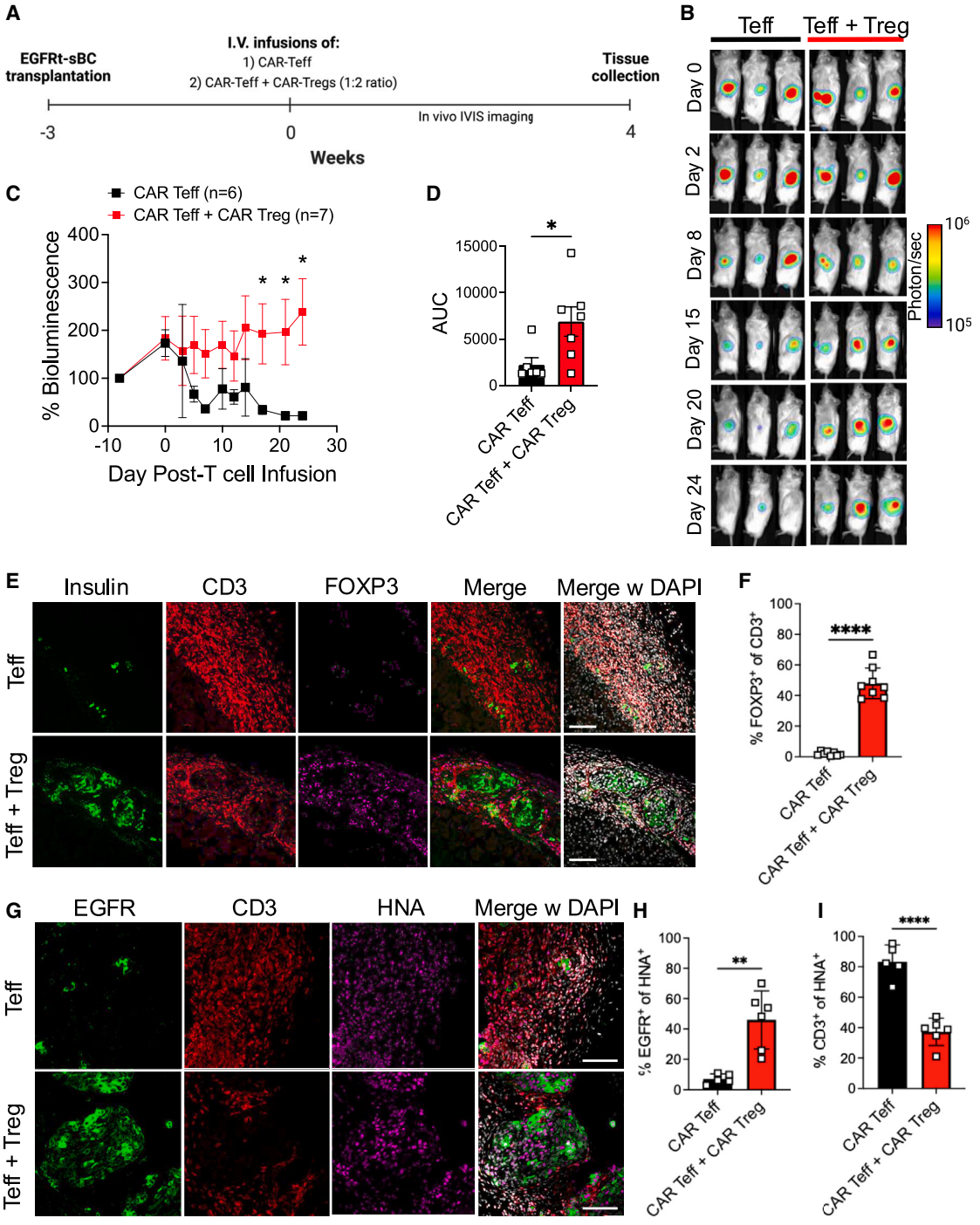

Figure 4. CAR-Tregs traffic to EGFRt-sBC grafts and suppress CAR-T effector cell-mediated graft destruction

(A) Schematic for transplantation study using EGFRt-sBC grafts and infusion of CAR-Teffs ± CAR-Tregs.

(B) *In vivo* luciferase imaging at different days post-T-cell infusion.

(C and D) Quantification of luciferase bioluminescence as a percentage of luciferase intensity before T cell infusion (C) and area under the curve (AUC) analysis (D) of the data. In (C), points represent mean and standard error of the mean. In (D), bars represent mean and standard error of the mean.

(E) Immunofluorescence (IF) staining of EGFRt-sBC grafts after T cell infusion for insulin (green), CD3 (red), FOXP3 (magenta), and DAPI (white). Scale bar represents 100 μm.

(F) Quantification of IF images in (E) for frequency of FOXP3$^+$ cells of total CD3$^+$ cells (n = 3 biological replicates with 2–3 different sections/tissue). Bars represent mean and standard deviation.

(G) IF staining of EGFRt-sBC grafts after T cell infusion for EGFR (green), CD3 (red), HNA (magenta), and DAPI (white). Scale bar represents 100 μm.

(legend continued on next page)

CAR-Tregs migrate to and protect transplanted HLA-A2-expressing cells from immune attack in preclinical models.[19,20,48] However, this approach cannot be utilized in patients with an HLA-A2 genotype, reducing its utility considerably.

Here, we utilized a CAR against human EGFR in conjunction with EGFRt as an inert ligand on hPSCs and hPSC-derived cells as a proof of concept for a combinatorial engineering strategy to provide localized immune suppression for sBC grafts.[20] We reason that, as EGFR is a naturally occurring non-polymorphic protein, EGFRt should not generate an immune reaction in patients. EGFRt can be effectively expressed in hPSCs, and its surface expression is maintained after differentiation into sBCs. Of note, differentiation efficiency was not altered compared to controls, excluding unwanted effects of the transgene for target tissue generation. Using multiple human donors, we demonstrate effective CAR expression in Treg populations at high efficiency. Importantly, autologous Tregs can be readily isolated and engineered *in vitro* before infusion back into the patient, providing a viable avenue for the translation of our strategy to the clinic. Also, CAR expression did not alter Treg stability or identity, key components of effective Treg inhibitory function.[51]

We demonstrated that CAR-Tregs are stimulated by the presence of EGFRt on target cells, including EGFRt-sBCs. Activated CAR-Tregs inhibited costimulatory receptor expression on DCs and suppressed Teff proliferation *in vitro*, highlighting the multifold immune modulation capabilities of Tregs. Most importantly, when EGFRt-sBCs were transplanted into immunodeficient mice, CAR-Tregs protected EGFRt-sBCs from CAR-Teff-mediated destruction. These data demonstrate that the genetic engineering of a unique, inert, otherwise not expressed surface protein on a stem cell-derived target tissue can be utilized to achieve localized CAR-Treg-mediated protection. While we use EGFRt as a proof-of-concept approach, this work will open doors for the development of other bait proteins in the future. Further studies are required to understand if this approach can inhibit polyclonal allogeneic and/or autoimmune-mediated graft rejection for applications across multiple disease contexts.

Collectively, this proof-of-concept study suggests that combinatorial genetic engineering can be utilized for the creation of off-the-shelf hPSCs and patient-derived CAR-Tregs to generate a localized immunosuppressive environment against a unique bait expressed in the hPSCs and their derivatives and in no other tissue. While this study assessed the effectiveness of this approach in the context of beta cell transplantation, this technique may be efficacious in a wide array of diseases that harness hPSC-derived tissues for regenerative medicine, such as skin grafts and organ transplantation. We further envision that this orthogonal technology will also be combined with other genetic alterations or inhibitory biomaterials to further improve transplant survival and may be able to synergize with or be a safer alternative to hypoimmunogenic cells for cell replacement therapies.

Limitations of the study

While the combinatorial genome engineering approach described here provides critical proof-of-concept data for our strategy to provide localized immune tolerance to stem cell-derived tissues, we acknowledge that the EGFR-CAR construct employed here is not specific for the EGFRt bait but also recognizes endogenous EGFR expressed by several tissues, reducing its immediate clinical relevance. Subsequent studies will investigate the use of specific CAR-bait pairings to overcome potential unspecific targeting of CAR-Tregs. We provide *in vitro* data on the suppressive capacity of CAR-Tregs on both innate and adaptive immune cells but focused the *in vivo* experiments on a recently described T cell-mediated rejection model without other human immune cells present.[20,41] While we believe our *in vitro* data demonstrating DC suppression are supportive of the idea that CAR-Tregs would be effective in suppressing immune responses in a broader manner, we cannot rule out the impact of other immune cell populations *in vivo*. This aspect of immune rejection warrants further study as better humanized mouse models become available but is currently outside of the scope of this manuscript. Further detailed experiments are also needed to understand the long-term survival, stability, and function of sBC grafts in a diabetic model with immune protection provided by CAR-Tregs using our dual engineering approach.

RESOURCE AVAILABILITY

Lead contact

Further information and requests for resources and reagents should be directed to and will be fulfilled by the lead contact, Leonardo M.R. Ferreira (ferreirl@musc.edu).

Materials availability

Any requests should be addressed to Leonardo M.R. Ferreira. Mel1 human embryonic stem cell (hESC) line (NIHhESC-11-0139) requires a material transfer agreement (MTA) with the University of Queensland, Australia, and a Stem Cell Research Oversight Committee (SCRO) registration number.

Data and code availability

Source data are available upon request. This paper does not report original code.

ACKNOWLEDGMENTS

Artwork in certain figures was created using BioRender.com. The work in the Ferreira and Russ laboratories is supported by Human Islet Research Network (HIRN) Emerging Leader in Type 1 Diabetes Grant #U24DK104162-07 to L.M.R.F., South Carolina Clinical and Translational Research (SCTR) Pilot Project Discovery Grant #1TL1TR001451-01 to L.M.R.F. and H.A.R., Diabetes Research Connection (DRC) grant IPF 22-1224 to L.M.R.F., R01DK12044 and R01DK132387 to H.A.R., a new investigator award from NIDDK/HIRN RRID: SCR_014393, UC24 DK104162 to H.A.R., SRA grants 2-SRA-2023-1313-S-B and 3-SRA-2023-1367-S-B by the Juvenile Diabetes Research Foundation (JDRF) to H.A.R., Advanced Postdoctoral Fellowship 3-APF-2024-1492-A-N by the JDRF to J.M.B., and the Thomas H. Maren Research Excellence Postdoctoral Award by UF to J.M.B. This work was also supported

(H and I) Quantification of IF images in (G) for the frequency of EGFR$^+$ cells (H) and CD3$^+$ cells (I) of total HNA$^+$ cells (n = 3 biological replicates with 1–2 different sections/tissue). Bars represent mean and standard deviation.

Data are from two independent cohorts with N = 13 total mice (B–D). Data are representative of at least two mice/group with multiple slides analyzed per mouse (E–I). Data were analyzed by unpaired t test. ns, not significant; *$p < 0.05$, **$p < 0.01$, and ****$p < 0.0001$.

in part by the Flow Cytometry and Cell Sorting Shared Resource, Hollings Cancer Center, Medical University of South Carolina (P30 CA138313).

AUTHOR CONTRIBUTIONS

J.M.B. designed experiments, conducted experiments, analyzed data, and wrote the manuscript. R.A.R. designed experiments, conducted experiments, and wrote the manuscript. R.C.-G. designed experiments and conducted experiments. J.P. conducted experiments. H.A.R. conceived the concept, supervised work, designed experiments, conducted experiments, and wrote the manuscript. L.M.R.F. supervised work, designed experiments, conducted experiments, and wrote the manuscript. The manuscript was edited and approved by all authors.

DECLARATION OF INTERESTS

A provisional patent on the strategy described in this article has been submitted with L.M.R.F. and H.A.R. as inventors. L.M.R.F. is an inventor in and has received royalties from patents on genetically modified human stem cells and T cells and consults for Guidepoint Global and McKesson. H.A.R. holds patents in the regenerative medicine space and served as a science advisory board (SAB) member of Sigilon Therapeutics and Prellis Biologics and consults or has consulted for Sigilon Therapeutics, Eli Lilly, Minutia, Guidepoint Global, Axon Advisors, and Tolerance Bio. H.A.R. is a scientific cofounder of Tolerance Bio.

STAR★METHODS

Detailed methods are provided in the online version of this paper and include the following:

- KEY RESOURCES TABLE
- EXPERIMENTAL MODEL AND STUDY PARTICIPANTS DETAILS
  - Human pluripotent stem cells (hPSCs)
  - Human pluripotent stem cell-derived beta cells
  - Human regulatory T cells (Tregs) and effector T cells (Teff)
  - Human monocyte-derived dendritic cells (moDCs)
  - Human myelogenous leukemia K562 cell lines
  - Humanized mouse model of type 1 diabetes
- METHOD DETAILS
  - TALEN-mediated genetic engineering of EGFRt and luciferase
  - Stem cell-derived beta cell (sBC) directed differentiation
  - Dynamic glucose stimulated insulin secretion
  - Molecular biology and CAR lentivirus production
  - Human T cell isolation and culture
  - CAR T cell transduction and expansion
  - *In vitro* CAR-Treg activation assay
  - Monocyte isolation and dendritic cell differentiation
  - *In vitro* dendritic cell suppression assay
  - *In vitro* T cell suppression assay
  - *In vitro* sBC cytotoxicity assay
  - Flow cytometry
  - sBC kidney capsule transplantation
  - *In vivo* bioluminescence imaging
  - Tissue processing
  - Histological analysis
  - Quantitative real-time PCR
- QUANTIFICATION AND STATISTICAL ANALYSIS
- ADDITIONAL RESOURCES

SUPPLEMENTAL INFORMATION

Supplemental information can be found online at https://doi.org/10.1016/j.celrep.2024.114994.

Received: December 11, 2023
Revised: October 7, 2024
Accepted: November 4, 2024
Published: November 18, 2024

REFERENCES

1. Monsarrat, P., Vergnes, J.N., Planat-Bénard, V., Ravaud, P., Kémoun, P., Sensebé, L., and Casteilla, L. (2016). An Innovative, Comprehensive Mapping and Multiscale Analysis of Registered Trials for Stem Cell-Based Regenerative Medicine. Stem Cells Transl. Med. *5*, 826–835. https://doi.org/10.5966/sctm.2015-0329.
2. Ettenger, R., Chin, H., Kesler, K., Bridges, N., Grimm, P., Reed, E.F., Sarwal, M., Sibley, R., Tsai, E., Warshaw, B., and Kirk, A.D. (2017). Relationship Among Viremia/Viral Infection, Alloimmunity, and Nutritional Parameters in the First Year After Pediatric Kidney Transplantation. Am. J. Transplant. *17*, 1549–1562. https://doi.org/10.1111/ajt.14169.
3. Nelson, J., Alvey, N., Bowman, L., Schulte, J., Segovia, M.C., McDermott, J., Te, H.S., Kapila, N., Levine, D.J., Gottlieb, R.L., et al. (2022). Consensus recommendations for use of maintenance immunosuppression in solid organ transplantation: Endorsed by the American College of Clinical Pharmacy, American Society of Transplantation, and the International Society for Heart and Lung Transplantation. Pharmacotherapy *42*, 599–633. https://doi.org/10.1002/phar.2716.
4. Shivaswamy, V., Boerner, B., and Larsen, J. (2016). Post-Transplant Diabetes Mellitus: Causes, Treatment, and Impact on Outcomes. Endocr. Rev. *37*, 37–61. https://doi.org/10.1210/er.2015-1084.
5. Schmidt, A., Oberle, N., and Krammer, P.H. (2012). Molecular mechanisms of treg-mediated T cell suppression. Front. Immunol. *3*, 51. https://doi.org/10.3389/fimmu.2012.00051.
6. Sakaguchi, S., Mikami, N., Wing, J.B., Tanaka, A., Ichiyama, K., and Ohkura, N. (2020). Regulatory T Cells and Human Disease. Annu. Rev. Immunol. *38*, 541–566. https://doi.org/10.1146/annurev-immunol-042718-041717.
7. Raffin, C., Vo, L.T., and Bluestone, J.A. (2020). T_{reg} cell-based therapies: challenges and perspectives. Nat. Rev. Immunol. *20*, 158–172. https://doi.org/10.1038/s41577-019-0232-6.
8. Bluestone, J.A., Buckner, J.H., Fitch, M., Gitelman, S.E., Gupta, S., Hellerstein, M.K., Herold, K.C., Lares, A., Lee, M.R., Li, K., et al. (2015). Type 1 diabetes immunotherapy using polyclonal regulatory T cells. Sci. Transl. Med. *7*, 315ra189. https://doi.org/10.1126/scitranslmed.aad4134.
9. Tang, Q., Leung, J., Peng, Y., Sanchez-Fueyo, A., Lozano, J.J., Lam, A., Lee, K., Greenland, J.R., Hellerstein, M., Fitch, M., et al. (2022). Selective decrease of donor-reactive T_{regs} after liver transplantation limits T(reg) therapy for promoting allograft tolerance in humans. Sci. Transl. Med. *14*, eabo2628. https://doi.org/10.1126/scitranslmed.abo2628.
10. Ghobadinezhad, F., Ebrahimi, N., Mozaffari, F., Moradi, N., Beiranvand, S., Pournazari, M., Rezaei-Tazangi, F., Khorram, R., Afshinpour, M., Robino, R.A., et al. (2022). The emerging role of regulatory cell-based therapy in autoimmune disease. Front. Immunol. *13*, 1075813. https://doi.org/10.3389/fimmu.2022.1075813.
11. Tarbell, K.V., Yamazaki, S., Olson, K., Toy, P., and Steinman, R.M. (2004). CD25+ CD4+ T cells, expanded with dendritic cells presenting a single autoantigenic peptide, suppress autoimmune diabetes. J. Exp. Med. *199*, 1467–1477. https://doi.org/10.1084/jem.20040180.
12. Noyan, F., Lee, Y.S., Hardtke-Wolenski, M., Knoefel, A.K., Taubert, R., Baron, U., Manns, M.P., and Jaeckel, E. (2013). Donor-specific regulatory T cells generated on donor B cells are superior to CD4+CD25high cells in controlling alloimmune responses in humanized mice. Transplant. Proc. *45*, 1832–1837. https://doi.org/10.1016/j.transproceed.2013.01.073.
13. Depil, S., Duchateau, P., Grupp, S.A., Mufti, G., and Poirot, L. (2020). 'Off-the-shelf' allogeneic CAR T cells: development and challenges. Nat. Rev. Drug Discov. *19*, 185–199. https://doi.org/10.1038/s41573-019-0051-2.
14. Sadelain, M., Brentjens, R., and Rivière, I. (2013). The basic principles of chimeric antigen receptor design. Cancer Discov. *3*, 388–398. https://doi.org/10.1158/2159-8290.CD-12-0548.
15. Davila, M.L., and Brentjens, R.J. (2016). CD19-Targeted CAR T cells as novel cancer immunotherapy for relapsed or refractory B-cell acute lymphoblastic leukemia. Clin. Adv. Hematol. Oncol. *14*, 802–808.

16. Cappell, K.M., and Kochenderfer, J.N. (2023). Long-term outcomes following CAR T cell therapy: what we know so far. Nat. Rev. Clin. Oncol. *20*, 359–371. https://doi.org/10.1038/s41571-023-00754-1.

17. Zhang, Q., Lu, W., Liang, C.L., Chen, Y., Liu, H., Qiu, F., and Dai, Z. (2018). Chimeric Antigen Receptor (CAR) Treg: A Promising Approach to Inducing Immunological Tolerance. Front. Immunol. *9*, 2359. https://doi.org/10.3389/fimmu.2018.02359.

18. Ferreira, L.M.R., Muller, Y.D., Bluestone, J.A., and Tang, Q. (2019). Next-generation regulatory T cell therapy. Nat. Rev. Drug Discov. *18*, 749–769. https://doi.org/10.1038/s41573-019-0041-4.

19. MacDonald, K.G., Hoeppli, R.E., Huang, Q., Gillies, J., Luciani, D.S., Orban, P.C., Broady, R., and Levings, M.K. (2016). Alloantigen-specific regulatory T cells generated with a chimeric antigen receptor. J. Clin. Invest. *126*, 1413–1424. https://doi.org/10.1172/JCI82771.

20. Muller, Y.D., Ferreira, L.M.R., Ronin, E., Ho, P., Nguyen, V., Faleo, G., Zhou, Y., Lee, K., Leung, K.K., Skartsis, N., et al. (2021). Precision Engineering of an Anti-HLA-A2 Chimeric Antigen Receptor in Regulatory T Cells for Transplant Immune Tolerance. Front. Immunol. *12*, 686439. https://doi.org/10.3389/fimmu.2021.686439.

21. Spanier, J.A., Fung, V., Wardell, C.M., Alkhatib, M.H., Chen, Y., Swanson, L.A., Dwyer, A.J., Weno, M.E., Silva, N., Mitchell, J.S., et al. (2023). Tregs with an MHC class II peptide-specific chimeric antigen receptor prevent autoimmune diabetes in mice. J. Clin. Invest. *133*, e168601. https://doi.org/10.1172/JCI168601.

22. Obarorakpor, N., Patel, D., Boyarov, R., Amarsaikhan, N., Cepeda, J.R., Eastes, D., Robertson, S., Johnson, T., Yang, K., Tang, Q., and Zhang, L. (2023). Regulatory T cells targeting a pathogenic MHC class II: Insulin peptide epitope postpone spontaneous autoimmune diabetes. Front. Immunol. *14*, 1207108. https://doi.org/10.3389/fimmu.2023.1207108.

23. Steffes, M.W., Sibley, S., Jackson, M., and Thomas, W. (2003). Beta-cell function and the development of diabetes-related complications in the diabetes control and complications trial. Diabetes Care *26*, 832–836. https://doi.org/10.2337/diacare.26.3.832.

24. Pepper, A.R., Bruni, A., and Shapiro, A.M.J. (2018). Clinical islet transplantation: is the future finally now? Curr. Opin. Organ Transplant. *23*, 428–439. https://doi.org/10.1097/MOT.0000000000000546.

25. Karimova, M.V., Gvazava, I.G., and Vorotelyak, E.A. (2022). Overcoming the Limitations of Stem Cell-Derived Beta Cells. Biomolecules *12*, 810. https://doi.org/10.3390/biom12060810.

26. Rezania, A., Bruin, J.E., Arora, P., Rubin, A., Batushansky, I., Asadi, A., O'dwyer, S., Quiskamp, N., Mojibian, M., Albrecht, T., et al. (2014). Reversal of diabetes with insulin-producing cells derived in vitro from human pluripotent stem cells. Nat. Biotechnol. *32*, 1121–1133.

27. Velazco-Cruz, L., Song, J., Maxwell, K.G., Goedegebuure, M.M., Augsornworawat, P., Hogrebe, N.J., and Millman, J.R. (2019). Acquisition of dynamic function in human stem cell-derived β cells. Stem Cell Rep. *12*, 351–365.

28. Russ, H.A., Parent, A.V., Ringler, J.J., Hennings, T.G., Nair, G.G., Shveygert, M., Guo, T., Puri, S., Haataja, L., Cirulli, V., et al. (2015). Controlled induction of human pancreatic progenitors produces functional beta-like cells in vitro. EMBO J. *34*, 1759–1772.

29. Castro-Gutierrez, R., Alkanani, A., Mathews, C.E., Michels, A., and Russ, H.A. (2021). Protecting Stem Cell Derived Pancreatic Beta-Like Cells From Diabetogenic T Cell Recognition. Front. Endocrinol. *12*, 707881. https://doi.org/10.3389/fendo.2021.707881.

30. Santini-Gonzalez, J., Castro-Gutierrez, R., Becker, M.W., Rancourt, C., Russ, H.A., and Phelps, E.A. (2022). Human stem cell derived beta-like cells engineered to present PD-L1 improve transplant survival in NOD mice carrying human HLA class I. Front. Endocrinol. *13*, 989815. https://doi.org/10.3389/fendo.2022.989815.

31. Micallef, S.J., Li, X., Schiesser, J.V., Hirst, C.E., Yu, Q.C., Lim, S.M., Nostro, M.C., Elliott, D.A., Sarangi, F., Harrison, L.C., et al. (2012). INS(GFP/w) human embryonic stem cells facilitate isolation of in vitro derived insulin-producing cells. Diabetologia *55*, 694–706. https://doi.org/10.1007/s00125-011-2379-y.

32. Docherty, F.M., Riemondy, K.A., Castro-Gutierrez, R., Dwulet, J.M., Shilleh, A.H., Hansen, M.S., Williams, S.P., Armitage, L.H., Santostefano, K.E., and Wallet, M.A. (2021). ENTPD3 marks mature stem cell derived beta cells formed by self-aggregation in vitro. Diabetes *70*, 2554–2567.

33. Siegel, E.G., Wollheim, C.B., Kikuchi, M., Renold, A.E., and Sharp, G.W. (1980). Dependency of cyclic AMP-induced insulin release on intra- and extracellular calcium in rat islets of Langerhans. J. Clin. Invest. *65*, 233–241. https://doi.org/10.1172/JCI109665.

34. Xia, L., Zheng, Z.Z., Liu, J.Y., Chen, Y.J., Ding, J.C., Xia, N.S., Luo, W.X., and Liu, W. (2020). EGFR-targeted CAR-T cells are potent and specific in suppressing triple-negative breast cancer both *in vitro* and *in vivo*. Clin. Transl. Immunology *9*, e01135. https://doi.org/10.1002/cti2.1135.

35. Butler, M.O., Ansén, S., Tanaka, M., Imataki, O., Berezovskaya, A., Mooney, M.M., Metzler, G., Milstein, M.I., Nadler, L.M., and Hirano, N. (2010). A panel of human cell-based artificial APC enables the expansion of long-lived antigen-specific CD4+ T cells restricted by prevalent HLA-DR alleles. Int. Immunol. *22*, 863–873. https://doi.org/10.1093/intimm/dxq440.

36. Fiorentino, D.F., Zlotnik, A., Mosmann, T.R., Howard, M., and O'Garra, A. (1991). IL-10 inhibits cytokine production by activated macrophages. J. Immunol. *147*, 3815–3822.

37. Brooks, D.G., Walsh, K.B., Elsaesser, H., and Oldstone, M.B.A. (2010). IL-10 directly suppresses CD4 but not CD8 T cell effector and memory responses following acute viral infection. Proc. Natl. Acad. Sci. USA *107*, 3018–3023. https://doi.org/10.1073/pnas.0914500107.

38. Minty, A., Chalon, P., Derocq, J.M., Dumont, X., Guillemot, J.C., Kaghad, M., Labit, C., Leplatois, P., Liauzun, P., Miloux, B., et al. (1993). Interleukin-13 is a new human lymphokine regulating inflammatory and immune responses. Nature *362*, 248–250. https://doi.org/10.1038/362248a0.

39. Zhu, C., Zhang, A., Huang, S., Ding, G., Pan, X., and Chen, R. (2010). Interleukin-13 inhibits cytokines synthesis by blocking nuclear factor-κB and c-Jun N-terminal kinase in human mesangial cells. J. Biomed. Res. *24*, 308–316. https://doi.org/10.1016/S1674-8301(10)60043-7.

40. Russell, M.A., Cooper, A.C., Dhayal, S., and Morgan, N.G. (2013). Differential effects of interleukin-13 and interleukin-6 on Jak/STAT signaling and cell viability in pancreatic beta-cells. Islets *5*, 95–105. https://doi.org/10.4161/isl.24249.

41. Ellis, C.E., Mojibian, M., Ida, S., Fung, V.C.W., Skovsø, S., McIver, E., O'Dwyer, S., Webber, T.D., Braam, M.J.S., Saber, N., et al. (2023). Human A2-CAR T Cells Reject HLA-A2 + Human Islets Transplanted Into Mice Without Inducing Graft-versus-host Disease. Transplantation *107*, e222–e233. https://doi.org/10.1097/TP.0000000000004709.

42. Crow, D. (2019). Could iPSCs Enable "Off-the-Shelf" Cell Therapy? Cell *177*, 1667–1669. https://doi.org/10.1016/j.cell.2019.05.043.

43. Han, X., Wang, M., Duan, S., Franco, P.J., Kenty, J.H.R., Hedrick, P., Xia, Y., Allen, A., Ferreira, L.M.R., Strominger, J.L., et al. (2019). Generation of hypoimmunogenic human pluripotent stem cells. Proc. Natl. Acad. Sci. USA *116*, 10441–10446. https://doi.org/10.1073/pnas.1902566116.

44. Hu, X., White, K., Olroyd, A.G., DeJesus, R., Dominguez, A.A., Dowdle, W.E., Friera, A.M., Young, C., Wells, F., Chu, E.Y., et al. (2024). Hypoimmune induced pluripotent stem cells survive long term in fully immunocompetent, allogeneic rhesus macaques. Nat. Biotechnol. *42*, 413–423. https://doi.org/10.1038/s41587-023-01784-x.

45. Deuse, T., Hu, X., Gravina, A., Wang, D., Tediashvili, G., De, C., Thayer, W.O., Wahl, A., Garcia, J.V., Reichenspurner, H., et al. (2019). Hypoimmunogenic derivatives of induced pluripotent stem cells evade immune rejection in fully immunocompetent allogeneic recipients. Nat. Biotechnol. *37*, 252–258. https://doi.org/10.1038/s41587-019-0016-3.

46. Gonzalez, B.J., Creusot, R.J., Sykes, M., and Egli, D. (2020). How Safe Are Universal Pluripotent Stem Cells? Cell Stem Cell *26*, 307–308. https://doi.org/10.1016/j.stem.2020.02.006.

47. James, E.A., Joglekar, A.V., Linnemann, A.K., Russ, H.A., and Kent, S.C. (2023). The beta cell-immune cell interface in type 1 diabetes (T1D). Mol. Metabol. *78*, 101809. https://doi.org/10.1016/j.molmet.2023.101809.

48. Rosado-Sanchez, I., Haque, M., Salim, K., Speck, M., Fung, V.C., Boardman, D.A., Mojibian, M., Raimondi, G., and Levings, M.K. (2023). Tregs integrate native and CAR-mediated costimulatory signals for control of allograft rejection. JCI Insight *8*, e167215. https://doi.org/10.1172/jci.insight.167215.

49. Riet, T., and Chmielewski, M. (2022). Regulatory CAR-T cells in autoimmune diseases: Progress and current challenges. Front. Immunol. *13*, 934343. https://doi.org/10.3389/fimmu.2022.934343.

50. Merkert, S., and Martin, U. (2016). Site-Specific Genome Engineering in Human Pluripotent Stem Cells. Int. J. Mol. Sci. *17*, 1000. https://doi.org/10.3390/ijms17071000.

51. Barbi, J., Pardoll, D., and Pan, F. (2014). Treg functional stability and its responsiveness to the microenvironment. Immunol. Rev. *259*, 115–139. https://doi.org/10.1111/imr.12172.

52. Gonzalez, F., Zhu, Z., Shi, Z.D., Lelli, K., Verma, N., Li, Q.V., and Huangfu, D. (2014). An iCRISPR platform for rapid, multiplexable, and inducible genome editing in human pluripotent stem cells. Cell Stem Cell *15*, 215–226. https://doi.org/10.1016/j.stem.2014.05.018.

53. Liu, W., Putnam, A.L., Xu-Yu, Z., Szot, G.L., Lee, M.R., Zhu, S., Gottlieb, P.A., Kapranov, P., Gingeras, T.R., Fazekas de St Groth, B., et al. (2006). CD127 expression inversely correlates with FoxP3 and suppressive function of human CD4+ T reg cells. J. Exp. Med. *203*, 1701–1711. https://doi.org/10.1084/jem.20060772.

54. Seddiki, N., Santner-Nanan, B., Martinson, J., Zaunders, J., Sasson, S., Landay, A., Solomon, M., Selby, W., Alexander, S.I., Nanan, R., et al. (2006). Expression of interleukin (IL)-2 and IL-7 receptors discriminates between human regulatory and activated T cells. J. Exp. Med. *203*, 1693–1700. https://doi.org/10.1084/jem.20060468.

55. Dawson, N.A.J., Rosado-Sanchez, I., Novakovsky, G.E., Fung, V.C.W., Huang, Q., McIver, E., Sun, G., Gillies, J., Speck, M., Orban, P.C., et al. (2020). Functional effects of chimeric antigen receptor co-receptor signaling domains in human regulatory T cells. Sci. Transl. Med. *12*, eaaz3866. https://doi.org/10.1126/scitranslmed.aaz3866.

56. McMurchy, A.N., and Levings, M.K. (2012). Suppression assays with human T regulatory cells: a technical guide. Eur. J. Immunol. *42*, 27–34. https://doi.org/10.1002/eji.201141651.

57. Szot, G.L., Koudria, P., and Bluestone, J.A. (2007). Transplantation of pancreatic islets into the kidney capsule of diabetic mice. J. Vis. Exp. *404*, 404. https://doi.org/10.3791/404.

58. Barra, J.M., Kozlovskaya, V., Kharlampieva, E., and Tse, H.M. (2020). Localized Immunosuppression With Tannic Acid Encapsulation Delays Islet Allograft and Autoimmune-Mediated Rejection. Diabetes *69*, 1948–1960. https://doi.org/10.2337/db20-0248.

59. Park, J.G., Na, M., Kim, M.G., Park, S.H., Lee, H.J., Kim, D.K., Kwak, C., Kim, Y.S., Chang, S., Moon, K.C., et al. (2020). Immune cell composition in normal human kidneys. Sci. Rep. *10*, 15678. https://doi.org/10.1038/s41598-020-72821-x.

STAR★METHODS

KEY RESOURCES TABLE

REAGENT or RESOURCE	SOURCE	IDENTIFIER
Antibodies		
TRA-1-60 (AF647) clone TRA-1-60-R	BioLegend	Cat#330606; RRID: AB_1227813
SOX2 (AF594) clone 114A6A34	BioLegend	Cat#656106; RRID: AB_2563431
SOX17 (AF488) clone P7-969	BD Biosciences	Cat#562205; RRID: AB_10893402
FOXA2 (PE) clone N17-280	BD Biosciences	Cat#561589; RRID: AB_10716057
Cleaved caspase 3 (AF647) clone C92-605	BD Biosciences	Cat#560626; RRID: AB_1727414
C-peptide (AF488) clone C-PEP-01	Origene	Cat#BM270; RRID: AB_978882
EGFR (PE) clone AY13	BioLegend	Cat#352904; RRID: AB_10896794
CD3ε (PE-Cy7) clone SK7	BioLegend	Cat#344816; RRID: AB_10640737
CD4 (FITC) clone SK3	BioLegend	Cat#980802; RRID: AB_2616621
CD4 (AF700) clone SK3	BioLegend	Cat#344621; RRID: AB_2563150
CD8 (PE) clone SK1	BioLegend	Cat#344706; RRID: AB_1953243
CD11c (FITC) clone 3.9	BioLegend	Cat#301603; RRID: AB_314174
CD25 (APC) clone BC96	BioLegend	Cat#302610; RRID: AB_314280
mCD45 (PE-Cy7) clone 30-F11	BioLegend	Cat#103114; RRID: AB_312979
CD69 (PE) clone FN50	BioLegend	Cat#310906; RRID: AB_314840
CD71 (FITC) clone CY1G4	BioLegend	Cat#334104; RRID: AB_1236432
CD80 (APC) clone 2D10	BioLegend	Cat#305220; RRID: AB_2291403
CD83 (BV421) clone HB15e	BioLegend	Cat#305324; RRID: AB_2561829
CD86 (PE) clone IT2.2	BioLegend	Cat#305406; RRID: AB_314526
CD127 (PE) clone A019D5	BioLegend	Cat#351304; RRID: AB_2564136
FOXP3 (eFluor 450) clone PCH101	eBioscience	Cat#48-4776-42; RRID: AB_1834364
HELIOS (PE) clone 22F6	BioLegend	Cat#137216; RRID: AB_10552903
NKX-6.1 (AF647) clone R11-560	BD Biosciences	Cat#563338; RRID: AB_2738144
PDX-1 (PE) clone 658A5	BD Biosciences	Cat#562161; RRID: AB_10893589
Anti-human insulin polyclonal	DAKO	Cat#A0564; RRID: AB_10013624
Anti-human PDX1 polyclonal	R&D Systems	Cat#AF2419; RRID: AB_355257
Anti-human NKX6.1 clone F55A10	Developmental Studies Hybridoma Bank	Cat#F55A10; RRID: AB_532378
Anti-human OCT3/4 clone C-10	Santa Cruz Biotechnology	Cat#Sc-5279; RRID: AB_628051
Anti-human EGFR polyclonal	R&D Systems	Cat#AF231; RRID: AB_355220
Anti-human NANOG polyclonal	Millipore Sigma	Cat#SAB2500670; RRID: AB_10602990
Anti-human FOXP3 clone 236A/E7	Abcam	Cat#ab20034; RRID: AB_445284
Anti-human CD3ε polyclonal	Abcam	Cat#ab5690; RRID: AB_305055
Anti-human HNA clone 235-1	Abcam	Cat#ab191181; RRID: AB_2885016
Anti-human Glucagon clone K79bb10	Millipore Sigma	Cat#G2654; RRID: AB_259852
Anti-human CK19 clone B974M	Aviva Systems Biology	Cat#OAMA02530; RRID: AB_204656415
Anti-human SOX9 polyclonal	Millipore Sigma	Cat#AB5535; RRID: AB_2239761
Anti-human SLC18A1 polyclonal	Millipore Sigma	Cat#HPA063797; RRID: AB_2685125
Bacterial and virus strains		
E. coli (NEB5-alpha; DH5α)	New England Biolabs	Cat#C2987I
Lentivirus for EGFR CAR and EGFRt	VectorBuilder	N/A

(*Continued on next page*)

Continued

REAGENT or RESOURCE	SOURCE	IDENTIFIER
Biological samples		
Human peripheral blood leukopak, fresh, tenth size	STEMCELL Technologies	Cat#200-0092
Chemicals, peptides, and recombinant proteins		
TrypLE	Gibco	Cat#12-604-021
Cultrex	Biotechne	Cat#3434-005-002
mTeSR+ media	STEMCELLTechnologies	Cat#05826
ITS	Gibco	Cat#41400-045
Activin A	R&D Systems	Cat#338-AC-01M
CHIR99021	STEMCELL Technologies	Cat#72054
KGF	Peprotech	Cat#100-19-1MG
D-Glucose	Gibco	Cat#11960-044
N-21 MAX	Biotechne	Cat#AR008
NEAA	Gibco	Cat#11140-050
Sodium Pyruvate	Gibco	Cat#11360-070
Sucrose	Sigma Aldrich	Cat#S0389-1KG
GlutaMAX	Gibco	Cat#35050-061
TTNPB	R&D Systems	Cat#0761
Sant-1	R&D Systems	Cat#1974
LDN	STEMCELL Technologies	Cat#72149
Paraformaldehyde (PFA)	ThermoFisher	Cat#28908
PMA	Sigma Aldrich	Cat#P1585-1MG
2-phospho-L-ascorbic acid trisodium salt (VitC)	Sigma	Cat#49752-10G
Heparin	Sigma	Cat#H3149-250KU
N-Acetyl-L-cysteine (Cysteine)	Sigma	Cat#A9165-25G
Zinc sulfate heptahydrate (Zinc)	Sigma	Cat#Z0251-100g
Alk5i II RepSox	R&D Systems	Cat#3742/50
3,3′,5-Triiodo-L-thyronine sodium salt (T3)	Sigma	Cat#T6397
Gamma Secretase Inhibitor XX (XXi)	AsisChem	Cat#ASIS-0149
Trace Elements A	Corning	Cat#25-021-CI
Critical commercial assays		
ELISA assay for human insulin	Alpco	80-INSHU-E10.1
Human CD4 isolation kit	STEMCELL Technologies	Cat#17952
Human CD8 isolation kit	STEMCELL Technologies	Cat#17953
Experimental models: Cell lines		
Human: Mel1$^{INS-GFP}$ ES cells	NIH registry: # 0139	N/A
Human: K562 cells	ATCC	Cat#CCL-243
Experimental models: Organisms/strains		
Mouse:NOD.Cg-*Prkdc*^{scid} *Il2rg*^{tm1Wjl}/SzJ Strain# 005557	Jackson Laboratories	RRID: IMSR_JAX:005557
Recombinant DNA		
EGFRt DNA fragment: sequence: 5′TCGTATAGCATACA TTATACGAAGTTATAATTCTGCAGATATGCTTCTCCTGG TGACAAGCCTTCTGCTCTGTGAGTTACCACACCCAGC ATTCCTCCTGATCCCACGCAAAGTGTGTAACGGAATA GGTATTGGTGAATTTAAAGACTCACTCTCCATAAATGC TACGAATATTAAACACTTCAAAAACTGCACCTCCATCA GTGGCGATCTCCACATCCTGCCGGTGGCATTTAGGG GTGACTCCTTCACACATACTCCTCCTCTGGATCCACA GGAACTGGATATTCTGAAAACCGTAAAGGAAATCACA GGGTTTTTGCTGATTCAGGCTTGGCCTGAAAACAGG ACGGACCTCCATGCCTTTGAGAACCTAGAAATCATAC	TWIST Bioscience	N/A

(*Continued on next page*)

Continued

REAGENT or RESOURCE	SOURCE	IDENTIFIER
GCGGCAGGACCAAGCAACATGGTCAGTTTTCTCTTG CAGTCGTCAGCCTGAACATAACATCCTTGGGATTACG CTCCCTCAAGGAGATAAGTGATGGAGATGTGATAATT TCAGGAAACAAAAATTTGTGCTATGCAAATACAATAAA CTGGAAAAAACTGTTTGGGACCTCCGGTCAGAAAAC CAAAATTATAAGCAACAGAGGTGAAAACAGCTGCAA GGCCACAGGCCAGGTCTGCCATGCCTTGTGCTCCCC CGAGGGCTGCTGGGGCCCGGAGCCCAGGGACTGCG TCTCTTGCCGGAATGTCAGCCGAGGCAGGGAATGCG TGGACAAGTGCAACCTTCTGGAGGGTGAGCCAAGGG AGTTTGTGGAGAACTCTGAGTGCATACAGTGCCACCC AGAGTGCCTGCCTCAGGCCATGAACATCACCTGCACA GGACGGGGACCAGACAACTGTATCCAGTGTGCCCACT ACATTGACGGCCCCCACTGCGTCAAGACCTGCCCGGC AGGAGTCATGGGAGAAAACAACACCCTGGTCTGGAAG TACGCAGACGCCGGCCATGTGTGCCACCTGTGCCATC CAAACTGCACCTACGGATGCACTGGGCCAGGTCTTGA AGGCTGTCCAACGAATGGGCCTAAGATCCCGTCCATC GCCACTGGGATGGTGGGGGCCCTCCTCTTGCTGCTGG TGGTGGCCCTGGGGATCGGCCTCTTCATGTGATTAAG ATACATTGATGAGTTTGGACAAACCACAACTAGAA 3′		
EGFRCAR-2A-mCherry: sequence:5′ATGGCCTTACCAG TGACCGCCTTGCTCCTGCCGCTGGCCTTGCTGCTCCA CGCCGCCAGGCCGGAGCAGAAGCTGATCAGCGAGGA GGACCTGCAGGTGCAGCTGAAACAGAGCGGCCCGGG CCTGGTGCAGCCGAGCCAGAGCCTGAGCATTACCTGC ACCGTGAGCGGCTTTAGCCTGACCAACTATGGCGTGC ATTGGGTGCGCCAGAGCCCGGGCAAAGGCCTGGAAT GGCTGGGCGTGATTTGGAGCGGCGGCAACACCGATT ATAACACCCCGTTTACCAGCCGCCTGAGCATTAACAA AGATAACAGCAAAAGCCAGGTGTTTTTTAAAATGAACA GCCTGCAGAGCAACGATACCGCGATTTATTATTGCGC GCGCGCGCTGACCTATTATGATTATGAATTTGCGTATT GGGGCCAGGGCACCCTGGTGACCGTGAGCGCGGGC GGCGGCGGCAGCGGCGGCGGCGGCAGCGGCGGCG GCGGCAGCGATATTCTGCTGACCCAGAGCCCGGTGAT TCTGAGCGTGAGCCCGGGCGAACGCGTGAGCTTTAGC TGCCGCGCGAGCCAGAGCATTGGCACCAACATTCATT GGTATCAGCAGCGCACCAACGGCAGCCCGCGCCTGCT GATTAAATATGCGAGCGAAAGCATTAGCGGCATTCCGAG CCGCTTTAGCGGCAGCGGCAGCGGCACCGATTTTACCC TGAGCATTAACAGCGTGGAAAGCGAAGATATTGCGGATT ATTATTGCCAGCAGAACAACAACTGGCCGACCACCTTTG GCGCGGGCACCAAACTGGAACTGAAAACCACGACGCC AGCGCCGCGACCACCAACACCGGCGCCCACCATCGCG TCGCAGCCCCTGTCCCTGCGCCCAGAGGCGTGCCGGC CAGCGGCGGGGGGCGCAGTGCACACGAGGGGGCTGG ACTTCGCCTGTGATTTTTGGGTGCTGGTGGTGGTTGGTG GAGTCCTGGCTTGCTATAGCTTGCTAGTAACAGTGGCCT TTATTATTTTCTGGGTGAGGAGTAAGAGGAGCAGGCTCC TGCACAGTGACTACATGAACATGACTCCCCGCCGCCCC GGGCCCACCCGCAAGCATTACCAGCCCTATGCCCCACC ACGCGACTTCGCAGCCTATCGCTCCTCGCGAAGAGTGA AGTTCAGCAGGAGCGCAGACGCCCCCGCGTACCAGCAG GGCCAGAACCAGCTCTATAACGAGCTCAATCTAGGACGA AGAGAGGAGTACGATGTTTTGGACAAGAGACGTGGCCGG GACCCTGAGATGGGGGGAAAGCCGAGAAGGAAGAACCC TCAGGAAGGCCTGTACAATGAACTGCAGAAAGATAAGATG GCGGAGGCCTACAGTGAGATTGGGATGAAAGGCGAGCG	VectorBuilder	N/A

(*Continued on next page*)

Continued

REAGENT or RESOURCE	SOURCE	IDENTIFIER
CCGGAGGGGCAAGGGGCACGATGGCCTTTACCAGGGTC TCAGTACAGCCACCAAGGACACCTACGACGCCCTTCACA TGCAGGCCCTGCCCCCTCGCGGAAGCGGAGAGGGCAG GGGAAGTCTTCTAACATGCGGGGACGTGGAGGAAAATCC CGGCCCCATGGTGAGCAAGGGCGAGGAGGATAACATGG CCATCATCAAGGAGTTCATGCGCTTCAAGGTGCACATGG AGGGCTCCGTGAACGGCCACGAGTTCGAGATCGAGGGC GAGGGCGAGGGCCGCCCCTACGAGGGCACCCAGACCG CCAAGCTGAAGGTGACCAAGGGTGGCCCCCTGCCCTTC GCCTGGGACATCCTGTCCCCTCAGTTCATGTACGGCTCC AAGGCCTACGTGAAGCACCCCGCCGACATCCCCGACTACTT GAAGCTGTCCTTCCCCGAGGGCTTCAAGTGGGAGCGCGTGAT GAACTTCGAGGACGGCGGCGTGGTGACCGTGACCCAGGACTC CTCCCTGCAGGACGGCGAGTTCATCTACAAGGTGAAGCTGCG CGGCACCAACTTCCCCTCCGACGGCCCCGTAATGCAGAAGAA GACCATGGGCTGGGAGGCCTCCTCCGAGCGGATGTACCCCGA GGACGGCGCCCTGAAGGGCGAGATCAAGCAGAGGCTGAAGC TGAAGGACGGCGGCCACTACGACGCTGAGGTCAAGACCACCT ACAAGGCCAAGAAGCCCGTGCAGCTGCCCGGCGCCTACAACGT CAACATCAAGTTGGACATCACCTCCCACAACGAGGACTACACC ATCGTGGAACAGTACGAACGCGCCGAGGGCCGCCACTCCACCGG CGGCATGGACGAGCTGTACAAGTAA 3′		
Plasmid: HR088 backbone plasmid	In-house[29,30]	N/A
Plasmid: Luciferase targeting	In-house[29,30]	N/A
Plasmid: AAVS1-TALEN-L	Gonzalez et al.[52]	Addgene #59025
Plasmid: AAVS1-TALEN-R	Gonzalez et al.[52]	Addgene #59026
Software and algorithms		
GraphPad Prism v10.2	GraphPad	N/A
BioRender	BioRender.com	N/A
FlowJo v10.10	FlowJo Portal	N/A
ImageJ	National Institutes of Health	N/A

EXPERIMENTAL MODEL AND STUDY PARTICIPANTS DETAILS

Human pluripotent stem cells (hPSCs)

Human pluripotent stem cell (hPSC) culture, maintenance, genome editing, and characterization were carried out as described in Methods Details and in accordance with the SCRO of the University of Florida and the Medical University of South Carolina.

Human pluripotent stem cell-derived beta cells

Wild-type and genome edited hPSC differentiation into stem cell-derived beta cells (sBCs) and characterization were carried out as described in method details.

Human regulatory T cells (Tregs) and effector T cells (Teff)

Regulatory T cell (Tregs) and effector T cel (Teff) isolation from human peripheral blood of de-identified (IRB-exempt) donors of different ages, ethnicities, body mass indices, and sexes, as well as culture, maintenance, genome editing, and characterization were carried out as described in method details.

Human monocyte-derived dendritic cells (moDCs)

Human monocyte isolation from human peripheral blood of de-identified (IRB-exempt) donors of different ages, ethnicities, body mass indices, and sexes, as well as differentiation into monocyte-derived dendritic cells (moDCs) and characterization were carried out as described in method details.

Human myelogenous leukemia K562 cell lines

K562 cells (a human myelogenous leukemia cell line) culture, genome modification, irradiation, and characterization were carried out as described in method details.

Humanized mouse model of type 1 diabetes

Male 8–12-week-old immunodeficient NOD-*scid* IL2Rg^{null} (NSG) mice were transplanted with genome edited hPSC-derived sBCs under the kidney capsule and subsequently challenged with engineered immune cells as described in Methods Details and in accordance to the IACUC of the Medical University of South Carolina (MUSC).

METHOD DETAILS

TALEN-mediated genetic engineering of EGFRt and luciferase

Undifferentiated human pluripotent stem cell (hPSC) Mel1$^{INS-GFP}$ line[31] were dissociated into single cells using TrypLE incubation at 37°C for 6 min. Digestion was then quenched with mTeSR+ media and cells counted using a Countess 3 cell counter (ThermoFisher Scientific). 2x10^6 cells were transferred into microcentrifuge tubes and washed with PBS. Washed cells were then prepared for nucleofection of Transcription Activator-Like Effector Nuclease (TALEN)-mediated knock-in (KI) of an EGFRt gene under control of a CAG promoter and a Firefly luciferase (Luc) gene under control of the endogenous AAVS1 promoter. Cells were nucleofected in P3 buffer per the Amaxa P3 Primary cell 4D-Nucleofector kit protocol (V4XP-3024) using the CB-150 program. AAVS1-TALEN-L and AAVS1-TALEN-R (a gift from Danwei Huangfu, Addgene plasmid #59025 and 59026) as well as CAG-EGFRt and Luc overexpression plasmids (generated in-house) were nucleofected into hPSC Mel1$^{INS-GFP}$ cells. Nucleofected cells were then plated in 10cm plates with 10 μM ROCK inhibitor (Y-27632, R&D Systems #1254-50) and SCR7. After 24 h, puromycin selection (0.5 μg/mL) was performed for 2 days followed by neomycin selection (50 μg/mL) for 6 days. Remaining colonies were picked and amplified for further characterization. Genomic DNA was extracted from targeted colonies and PCR analysis for TALEN KI was performed to identify successfully modified clones.

Stem cell-derived beta cell (sBC) directed differentiation

Undifferentiated human pluripotent stem (hPSC) Mel1$^{INS-GFP}$ reporter cells were maintained on human embryonic stem cell (hESC) qualified Cultrex (Biotechne #3434-005-002) in mTeSR+ media (STEMCELL Technologies #05826). Differentiation to stem cell-derived beta-like cells (sBC) was carried out in a suspension-based, bioreactor magnetic stirring system (Reprocell #ABBWVS03A-6, #ABBWVDW-1013, #ABBWBP03N0S-6), as previously described.[29,30] Briefly, 90% confluent hPSC cultures were dissociated into single-cell suspension by incubation with TrypLE (Gibco #12-604-021). Dissociation was halted with mTESR+ media, and cells were counted using a Countess 3 cell counter (ThermoFisher Scientific), followed by seeding 0.5 × 10^6 cells/mL in mTeSR+ media supplemented with 10 μM ROCK inhibitor in bioreactors. 3D sphere formation was performed for 48 h followed by induction of definitive endoderm differentiation using **d1 media** [RPMI containing 0.2% FBS, 1:5,000 ITS (Gibco #41400-045), 100 ng/mL Activin A (R&D Systems #338-AC-01M), and 3 μM CHIR99021 (STEMCELL Technologies #72054)]. Differentiation media was changed daily by letting spheres settle by gravity for 3-10min. Most supernatant was removed by aspiration; fresh media was added, and bioreactors were placed back on stirrer system. sBC differentiation was based on our published protocol[28] with modifications as outlined below. Differentiation medias are as: **day 2-3**: RPMI containing 0.2% FBS, 1:2,000 ITS, and 100 ng/mL Activin A; **d4-5**: RPMI containing 2% FBS, 1:1,000 ITS, and 50 ng/mL KGF (Peprotech #100-19-1MG); **d6**: DMEM with 4.5 g/L D-glucose (Gibco #11960-044) containing 1:50 *N*-21 MAX (Biotechne #AR008), 1:100 NEAA (Gibco #11140-050), 1mM Sodium Pyruvate (Gibco #11360-070), 1:100 GlutaMAX (Gibco #35050-061), 3 nM TTNPB, (R&D Systems #0761), 250 nM Sant-1 (R&D Systems #1974), 250 nM LDN (STEMCELL Technologies #72149), 30 nM PMA (Sigma Aldrich #P1585-1MG), 50 μg/mL 2-phospho-L-ascorbic acid trisodium salt (VitC) (Sigma #49752-10G); **d7**: DMEM containing 1:50 *N*-21 MAX, 1:100 NEAA, 1 mM Sodium Pyruvate, 1:100 GlutaMAX, 3 nM TTNPB, and 50 μg/mL VitC; **d8-9**: DMEM containing 1:50 *N*-21 MAX, 1:100 NEAA, 1 mM Sodium Pyruvate, 1:100 GlutaMAX, 100 ng/mL EGF (R&D Systems #236-EG-01M), 50 ng/mL KGF, and 50 μg/mL VitC; **d10-15**: DMEM containing 2% fraction V BSA, 1:100 NEAA, 1 mM Sodium Pyruvate, 1:100 GlutaMAX, 1:100 ITS, 10 μg/mL Heparin (Sigma #H3149-250KU), 2 mM N-Acetyl-L-cysteine (Cysteine) (Sigma #A9165-25G), 10 μM Zinc sulfate heptahydrate (Zinc) (Sigma #Z0251-100g), 1x BME, 10 μM Alk5i II RepSox (R&D Systems #3742/50), 1 μM 3,3′,5-Triiodo-L-thyronine sodium salt (T3) (Sigma #T6397), 0.5 μM LDN, 1uM Gamma Secretase Inhibitor XX (XXi) (AsisChem #ASIS-0149) and 1:250 1 M NaOH to adjust pH to ~7.4; **d16-30**: CMRL (Gibco #11530-037) containing 1:50 *N*-21 MAX, 1:100 NEAA, 1:100 GlutaMAX, 10ug/ml Heparin, 2mM Cysteine, 10 μM Zinc, 1x BME, 1 μM T3, 10 μM Alk5i II RepSox, 50ug/ml VitC, 1:1000 Trace Elements A (Corning # 25-021-CI), and 1:250 NaOH to adjust pH to ~7.4. All media also contained 1x Penicillin-Streptomycin.

Dynamic glucose stimulated insulin secretion

Dynamic insulin secretion was measured using a BioRep Technologies perifusion machine (PERI4-115-1810-076). 50 sBC clusters were placed on a filter in the perifusion chamber and various solutions were perfused through the system at 100 μL/min by a peristaltic pump; cells and solutions were kept at 37°C and ambient atmosphere. The perifusion program consisted of a 60-min pre-incubation step with KRB buffer containing low (2.8 mM) glucose followed by the following run program: 30 min low glucose, 15 min high (16.7 mM) glucose, 15 min high glucose + IBMX (50 μM), 10 min low glucose, 10 min KCl (30 mM), 10 min low glucose. Perifusion flow-through was collected in 96-well plates and stored at 4°C overnight or −20°C if longer storage was needed for future analysis. Cell pellets were recovered from the chamber after perifusion and lysed with acid/ethanol solution and frozen overnight before use for assessment of total insulin content.

Molecular biology and CAR lentivirus production

An epidermal growth factor receptor (EGFR) specific chimeric antigen receptor (CAR) gene was created by generating a chimeric DNA sequence encoding a signal peptide (SP) and Myc-tag upstream of an anti-EGFR scFv,[34] a CD8 hinge (H), CD28 transmembrane domain (TM), and a CD28^{-}CD3zeta tandem signaling domain. The CAR gene was linked to an upstream EF1α promoter sequence and a downstream mCherry reporter gene via a 2A self-cleaving peptide sequence. The EGFR CAR construct DNA was synthesized and subcloned in a lentiviral backbone by VectorBuilder (Chicago, IL). CAR lentivirus was produced, concentrated, frozen, and shipped by VectorBuilder to our lab, where it was kept in single use aliquots at -80°C until used.

Human T cell isolation and culture

Human peripheral blood leukopaks from de-identified healthy donors were purchased from STEMCELL Technologies (Vancouver, Canada), which collects and distributes de-identified human blood products with consent forms, according to protocols approved by the Institutional Review Board (IRB). CD4^{+} T cells and CD8^{+} T cells were purified using the EasySep Human CD4^{+} T cell Isolation Kit and the Human CD8^{+} T cell Isolation Kit, respectively (both from STEMCELL Technologies) as per manufacturer's instructions. Enriched CD4^{+} T cells were then stained for CD4, CD25, and CD127, and CD4^{+}CD25^{high}CD127^{low} regulatory T cells (Tregs), previously shown to be *bona fide* Tregs,[53,54] and CD4^{+}CD25^{low}CD127^{high} effector T cells (Teff) were sorted by fluorescence-assisted cell sorting (FACS) using a BD FACS Aria II Cell Sorter (Beckton Dickinson, Franklin Lakes, NJ). Post-sort analyses confirmed greater than 99% purity. T cells were counted with Trypan Blue using a TC20 Automated Cell Counter (BioRad, Hercules, CA), activated with anti-CD3/CD28 beads (Gibco, ThermoFisher Scientific) at a 1:1 ratio and recombinant human IL-2 (rhIL-2, Peprotech, ThermoFisher Scientific, Waltham, MA) and expanded in RPMI1640 medium supplemented with 10% fetal bovine serum (FBS), 1% Penicillin-Streptomycin, 2 mM GlutaMax, 10 mM HEPES, 1x non-essential amino acids (NEAA), and 1 mM sodium pyruvate (all from Gibco, ThermoFisher Scientific). Tregs were cultured with 1,000 IU/mL rhIL-2, CD4^{+} Teff cells with 100 IU/mL rhIL-2, and CD8^{+} T cells with 300 IU/mL rhIL-2. Antibodies and dyes used for FACS and for flow cytometry can be found in Table S1.

CAR T cell transduction and expansion

Two days after activation, T cells were transduced with EGFR CAR lentivirus at a multiplicity of infection (MOI) of 1 (1 particle per cell) with rhIL-2. After adding the EGFR CAR lentivirus, T cells were centrifuged at 1,000 g at 32°C for 1 h. Following transduction, T cells were maintained and expanded in RPMI10 medium with fresh medium and rhIL-2 being given every two days. Transduction efficiency was assessed by flow cytometry based on reporter mCherry expression.

In vitro CAR-Treg activation assay

CAR-Tregs were co-cultured with EGFRt-expressing target cells or anti-CD3/CD28 beads at a 1:1 ratio in RPMI10 medium supplemented with 1,000 IU/mL rhIL-2. Surface expression of early activation marker CD69 was assessed at 24 h, while surface expression of early/mid activation markers CD25 and CD71 was assessed at 48 h by flow cytometry.

Monocyte isolation and dendritic cell differentiation

Human CD14^{+} monocytes were enriched from leukopaks using the EasySep Human CD14^{+} Positive Selection Kit (STEMCELL Technologies) and differentiated into monocyte-derived dendritic cells (moDCs) using the ImmunoCult Dendritic Cell Culture Kit (STEMCELL Technologies), as per manufacturer's instructions. Complete moDC maturation was assessed by surface expression of CD11c, CD80, CD83, and CD86 using flow cytometry. Cells were frozen in aliquots in freezing medium (90% FBS, 10% DMSO) and stored in liquid nitrogen until being thawed for assays.

In vitro dendritic cell suppression assay

Modulation of monocyte-derived dendritic cells (moDC) by Tregs was performed as described before, with modifications.[55] Briefly, moDCs were thawed on the day of the experiment and plated in each well supplemented with 50 ng/mL IFNγ (STEMCELL Technologies) for overnight activation. In parallel, Tregs were activated, as described before. The next day, IFNγ was washed off from moDCs, then Tregs were co-cultured with moDCs for 3 days. Co-cultures were then harvested and stained with CD4, CD11c, CD80, CD83, and CD86. Suppression of moDC was gauged based on the surface expression level of CD80 and CD86.

In vitro T cell suppression assay

Inhibition of T cell proliferation by Tregs was assessed as described before, with modifications.[56] Responder T cells (Tresp, a 1:1 mixture of CAR CD4^{+}/CD8^{+} T cells) were labeled with CellTrace Far Red (CTFR) according to manufacturer's instructions (Invitrogen, ThermoFisher Scientific) and co-incubated with EGFRt-expressing sBC and CAR-Tregs at different Treg:Tresp ratios for 4 days. Co-cultures were then harvested and stained with CD4 and CD8. Percent suppression of T cell proliferation was calculated using

$$\%\ Suppression = \left[1 - \left(\frac{DI_{sample}}{DI_{max}}\right)\right] * 100$$

where DI stands for division index, the average number of cell divisions that a cell in the original Tresp population has undergone, as calculated in FlowJo v10.9 software (BD Life Sciences, Franklin Lakes, NJ).

In vitro sBC cytotoxicity assay

Cytotoxicity toward sBC was assessed by detection of cleaved caspase 3 (CASP3) expression in sBC using flow cytometry. Briefly, 50,000 sBCs were plated onto Cultrex-coated wells of a 96-well flat bottom plate in sBC medium and allowed to adhere at 37°C for 2 h. Then, sBCs were co-cultured with UT Tregs, UT Teff cells, CAR Tregs or CAR-Teff cells at a 1:1 ratio in RPMI10 medium supplemented with 100 IU/mL rhIL-2 (Teffs) or 1,000 IU/mL rhIL-2 (Tregs) for 48 h. Cells were harvested using TrypLE, stained for CD3 and cleaved caspase 3, and analyzed by flow cytometry.

Flow cytometry

For immune cells, master mixes for surface markers and intracellular markers were prepared for cells in FACS tubes or plates. For surface marker staining, cell culture supernatant was removed by centrifugation and pellets were re-suspended in 100 μL of master mix, then stained on ice for 30 min, protected from light. Cells were washed with 500 μL PBS and centrifuged to remove unbound/excess antibodies. For intracellular staining of markers, cells were fixed and permeabilized with the FOXP3/Transcription Factor Staining Kit (eBioscience 00-5523-00) after surface staining, according to manufacturer's instructions. For intracellular staining, cells were stained in 1x Permeabilization Buffer with antibodies for 30 min at room temperature, protected from light. Cells were then washed with 500 μL 1x Permeabilization Buffer and centrifuged to remove unbound/excess antibodies. Pellets were re-suspended in 200 μL PBS for analysis on a 5-laser CytoFlex (Beckman Coulter, Brea, CA) flow cytometer or a 3-laser Northern Lights (Cytek Biosciences, Fremont, CA) spectral flow cytometer. Single color compensation or references were prepared using matched cells or UltraComp eBeads Plus Compensation Beads (Invitrogen, ThermoFisher Scientific). Samples were acquired by recording at least 50,000 events, if appropriate, or 3 to 5 min acquisition time per tube.

For hPSC (i) and sBC (ii), single cell suspensions were made by (i) incubation with TrypLE (Gibco #12-604-021) for 8 min at 37°C. Detached cells were quenched with mTeSR+ media. (ii) hPSC or sBC clusters were washed with PBS and incubated with 0.05% Trypsin with EDTA at 37°C for (i) 3 min or (ii) 12 min to create a single cell suspension. Cells were quenched with 2% FBS in PBS and filtered using a cell strainer into 5mL FACS tubes and incubated for 30 min on ice for surface markers or fixed with 4% paraformaldehyde for 5 min at room temperature and stained in CAS buffer with 0.4% Triton X- overnight at 4°C for intracellular markers. After incubation, the cells were washed and resuspended in FACS buffer for analyses on 5-laser Cytek Aurora spectral flow cytometer. Analysis and graphs were made using FlowJo software v10.9 (BD Life Sciences).

A list of antibodies and dyes used can be found in Table S1.

sBC kidney capsule transplantation

Stem cell-derived beta cells (sBC) were transplanted into the kidney capsule of NOD-*scid* IL2Rg^{null} (NSG) mice as previously described[57,58] with modifications, as approved by MUSC's IACUC. Mice were first anesthetized with isoflurane, followed by lubricant application on the eyes and subcutaneous injections of analgesics (buprenorphine and meloxicam). After shaving and applying Nair, the surgical area was sterilized with povidone-iodine and alcohol swabs. The surgery was then performed aseptically, first by making an incision in the skin and then in the peritoneal layer. The kidney was then exposed and 500 sBC transplanted into the kidney capsule. The kidney was returned to its original position, the peritoneal incision closed with surgical stitches, and the skin incision closed with surgical clips. Experimental animals were monitored and received additional subcutaneous injections of analgesics in the following days, as per approved MUSC's IACUC protocol.

In vivo bioluminescence imaging

D-luciferin, potassium salt (GoldBio, St Louis, MO) was dissolved in DPBS (no calcium or magnesium) to a final concentration of 15 mg/mL and 0.22 μm filter sterilized. Mice were intraperitoneally injected with 100 mL D-luciferin solution and, 8 min later, imaged using an AMI optical imaging system (Spectral Instruments Imaging, Tucson, AZ) under isoflurane anesthesia for 60 s, two to three times a week. Luciferase activity data analysis was performed using Aura software (Spectral Instruments Imaging).

Tissue processing

Spleen and kidney samples were retrieved from humanely euthanized mice, according to MUSC's IACUC protocol, and processed. Spleens were mechanically homogenized into a single cell suspension with a 70 μm cell strainer and contaminating erythrocytes were lysed with ACK lysis buffer (Gibco, ThermoFisher Scientific). Kidneys were minced and digested with 1 mg/mL Collagenase D (Roche) in a heated OctoMacs dissociator (Miltenyi Biotec, Gaithersburg, MD) using the multi-tissue dissociator kit program settings, as previously described.[59]

Histological analysis

For immunofluorescence imaging of cell cultures, EGFRt or control WT hPSC were plated on Cultrex coated glass coverslips as described above. Cells were then fixed with 4% PFA for 10 min at room temperature, washed with 1x PBS, and incubated with primary antibodies overnight at 4°C (Table S2). AF488-, AF555-, or AF647-conjugated donkey anti-guinea pig, anti-mouse, or anti-goat IgG secondary antibodies (1:500, Jackson ImmunoResearch Laboratories) were used for detection. Coverslips were mounted on histology slides using Prolong Gold antifade reagent with DAPI (Invitrogen). Slides were imaged using a Zeiss inverted microscope (Zeiss) and the images were processed by Zeiss black software version 1.12. For immunofluorescence imaging of sBC graft tissue

slices, the sBC graft-containing kidney was retrieved from humanely euthanized mice, according to MUSC's IACUC protocol and fixed in 7 mL 4% paraformaldehyde (PFA) at room temperature for 2 h. The graft-containing kidney was then cut in half perpendicular to the graft without touching the graft and incubated in 7 mL 4% PFA for an additional hour at 4°C. The sliced fixed graft-containing kidney was then transferred to 5 mL 30% sucrose solution and incubated overnight at 4°C. The following day, the kidney halves were mounted in OCT medium in a cryomold and frozen on top of dry ice. OCT blocks were stored at −80°C until being sectioned and stained with antibodies (Table S2). Quantification of IF images was done using ImageJ (National Institutes of Health, Bethesda, MD). Steps to extract the necessary data included Remove Background (Process>Subtract Background; using 12 pixel rolling ball radius), then converting the image to 8-bit black and white (Image>Type>8-bit) to be able to adjust the threshold and remove the noise (Image>Adjust>Threshold). From there, cells were isolated in a two-step process: Process>Binary>Fill in Holes, then Process>Binary>Watershed. Finally, the function Analyze>Analyze Particles was used with the following parameters: size: 80 pixels-500 pixels; circularity: 0–1.

Quantitative real-time PCR

Total RNA was isolated using a micro RNeasy kit (QIAGEN, no. 74104) and reverse transcribed using the iSCRIPT cDNA kit (Bio-Rad, no. 1708891) as per the manufacturer's instructions. qPCR analysis was performed on a Bio-Rad CFX96 Touch Real-Time PCR Detection System using TaqMan probes and custom primers (Table S3). Data were set relative to *TBP* and plotted as the mean ± standard error of the mean (SEM).

QUANTIFICATION AND STATISTICAL ANALYSIS

Statistical details of each experiment can be found in the respective figure legend, including the statistical tests used, value of n, what n represents (e.g., number of mice or number of tissue sections), and dispersion and precision measures (e.g., mean, SD, SEM). Significance was defined as p-value less than 0.05 using the appropriate statistical test. No statistical methods were used to determine strategies for randomization or to estimate sample size. No data were excluded. Statistical analyses were performed using GraphPad Prism v10.0.0 (GraphPad Software, La Jolla, CA).

ADDITIONAL RESOURCES

Holger Russ's Laboratory Website: https://www.russlab.com and https://pharmacology.med.ufl.edu/research-2/the-russ-lab/
Leonardo Ferreira's Laboratory Website: https://www.ferreiralab.com/.